

CASE
COPY

NASA TN D-1199



TECHNICAL NOTE

D-1199

THREE-DIMENSIONAL SPHERE-OF-INFLUENCE ANALYSIS
OF INTERPLANETARY TRAJECTORIES TO MARS

By Gerald Knip, Jr., and Charles L. Zola

Lewis Research Center
Cleveland, Ohio

NATIONAL AERONAUTICS AND SPACE ADMINISTRATION
WASHINGTON

May 1962

1. The first part of the document is a title page. It contains the title of the document, the author's name, and the date of the document. The title is "The History of the United States of America". The author is "John Adams". The date is "1776".

2. The second part of the document is a preface. It contains the author's introduction to the document. The author states that the document is a history of the United States of America, and that it is written for the purpose of informing the public of the events that have shaped the nation.

3. The third part of the document is the main body of the text. It contains the author's account of the events that have shaped the United States of America. The author begins with the founding of the nation, and then proceeds to describe the various events that have shaped the nation's history, including the American Revolution, the Civil War, and the Reconstruction era.

NATIONAL AERONAUTICS AND SPACE ADMINISTRATION

TECHNICAL NOTE D-1199

THREE-DIMENSIONAL SPHERE-OF-INFLUENCE ANALYSIS
OF INTERPLANETARY TRAJECTORIES TO MARS

By Gerald Knip, Jr., and Charles L. Zola

SUMMARY

A method of analysis is presented for use in interplanetary trajectory studies which are essential to complete mission studies. The method employs arbitrary spheres about each planet that serve to differentiate planetocentric and heliocentric motion. The overall trajectory is composed of three trajectory segments - two planet-centered segments and one Sun-centered. A continuous coast path is formed by matching the coordinates of each of the planetocentric segments with those of the heliocentric segment at the respective spheres of influence. This method has been used to study the planetocentric and heliocentric segments of one-way trajectories from Earth to Mars. For a trip of fixed duration, planetocentric parameters such as inclination of escape plane, inclination of encounter plane, injection trajectory angle, arrival trajectory angle, and injection time were varied to determine their effects on injection-point location and mission velocity-increment requirements. Trips of 150-, 225-, and 300-day duration were used to investigate the relations among velocity-increment requirements, departure date, trip time, communication distance, heliocentric transfer-plane inclination, and synodic period of departure.

For a 1-day span in injection time, values of the planetocentric parameters can be selected to favor specific mission requirements, such as the use of available tracking stations or the avoidance of intense regions of the Van Allen belts, with only a slight penalty in velocity-increment requirements.

Because of planetary orbit eccentricities, the synodic period of departure has a pronounced effect on velocity-increment requirements and on arrival communication distance. Therefore, the use of circular-coplanar planetary orbit data is not recommended in specific Earth-to-Mars mission studies.

INTRODUCTION

Trajectory studies are essential to the planning of any space mission. In order to obtain a precise trajectory that could be used in final guidance and control settings for a specific flight, n-body calculations must be made. This procedure is, however, very cumbersome and does not lend itself to the broad parametric-type survey required for preliminary mission studies. Therefore, a multiple two-body method of analysis has been developed that is characterized by elliptical, noncoplanar (three-dimensional) planetary orbits. The method of analysis employs spheres of influence about the planets. The three required trajectory segments - two planet-centered segments and one Sun-centered - are matched in their coordinates at the spheres of influence to form a continuous path from an injection point near Earth to an arrival point near the destination planet. This procedure differs from that used in references 1 to 5 principally in the relation of the heliocentric segment of the trajectory to the planetocentric segments. In the "three-center" method of references 1 to 5, the heliocentric segment is independent of the other segments. In the sphere-of-influence method of the present report, the three segments are interdependent. Therefore, the "three-center" method is restricted to the heliocentric portion of an interplanetary trajectory, while the present method can be used to investigate the effects of planetocentric parameters on the overall interplanetary trajectory.

To illustrate the accuracy of the sphere-of-influence method, results for two representative trajectories from Earth to Mars are compared with the results of n-body calculations.

The effects, on a 300-day Earth-to-Mars trajectory, of changes in the planetocentric segments were studied. The interrelation among the following planetocentric parameters is discussed: injection time, injection-point longitude and latitude, injection- and arrival-velocity azimuths, escape- and encounter-plane inclination, and velocity-increment (ΔV) requirements.

One-way trajectories from Earth to Mars were investigated to study the three-dimensional problem with respect to ΔV , heliocentric transfer-plane inclination, trip time, communication distance, injection or departure date, and synodic period of departure. These data are compared with results of reference 6, which are characterized by circular-coplanar planetary orbits.

ANALYSIS

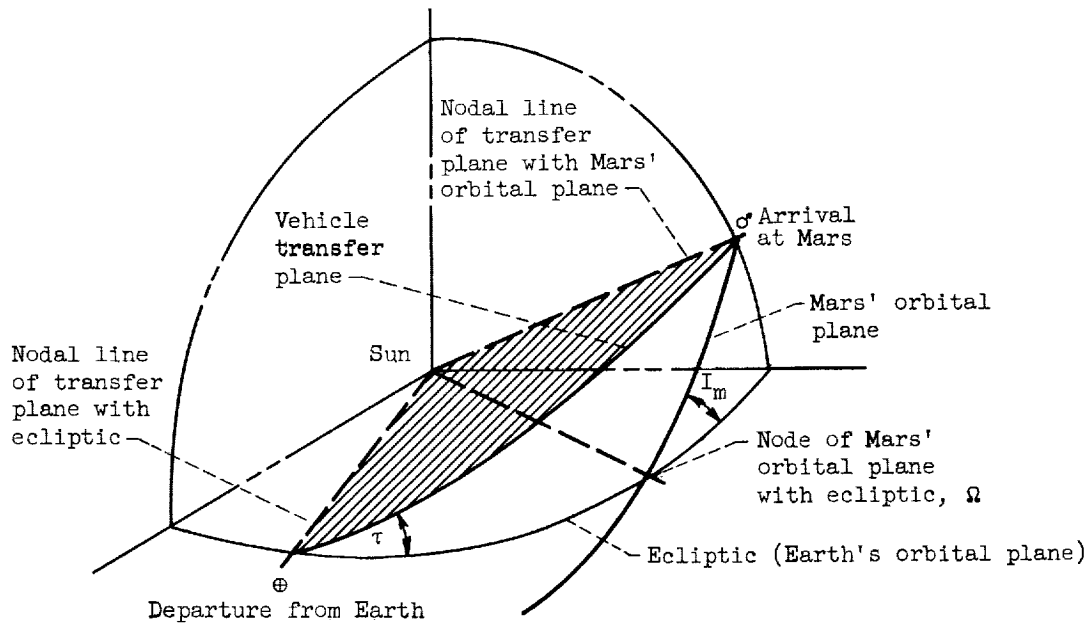
The spheres-of-influence model employed in calculating interplanetary trajectories consists of a three-dimensional solar system having

mutually inclined elliptical planetary orbits (sketch (a)). The arbitrary spheres about each planet serve as a boundary, inside of which it is assumed the vehicle is acted upon only by the inverse-square central force field of the planet. Outside the spheres of influence it is assumed the vehicle is acted upon only by the inverse-square central force field of the Sun. A typical interplanetary trajectory is composed of three distinct coast trajectory segments: the geocentric escape hyperbola, the heliocentric trajectory segment, and the planetocentric encounter hyperbola. For purposes of calculating energy (ΔV) requirements, it is assumed that all trips start and end in circular orbit. An impulsive thrust is assumed on injection at 1.1 Earth radii (perigee of the escape hyperbola) to initiate the coast phase of the interplanetary trip. Upon arrival at the perigee of the encounter hyperbola (1.1 Mars radii), an impulsive thrust is assumed to establish a circular parking orbit.

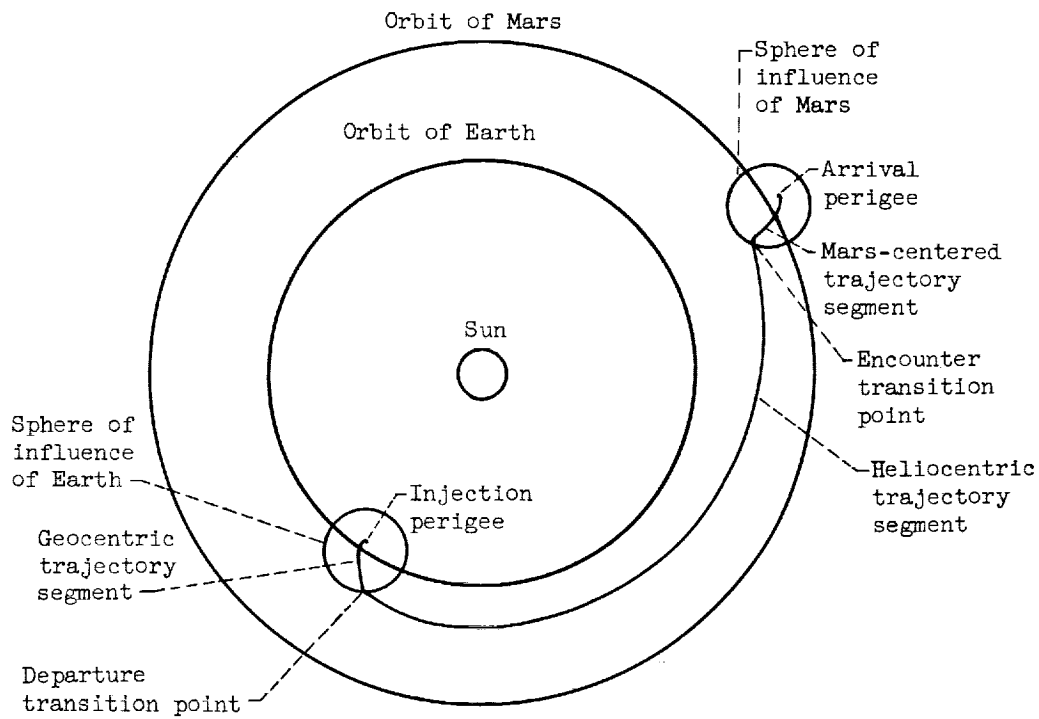
Positions of bodies are usually referenced to one of two systems of coordinates, the ecliptic system or the equatorial system. The fundamental planes are the ecliptic plane (plane of Earth's orbit) and equatorial plane (plane of the Earth's equator), respectively. The polar coordinates in the ecliptic system are called longitude and latitude; and in the equatorial, right ascension and declination. The present method uses the equatorial system for the geocentric portion of the analysis and the ecliptic for the heliocentric segment.

The symbols used in this study are given in appendix A, while the equations for the method of analysis are given in appendix B. An IBM 704 digital computer was used to perform the computations. Initial conditions required for a typical machine calculation are:

- (1) Escape and encounter hyperbola perigee radii
- (2) Perigee injection time
- (3) Perigee-to-perigee trip time, T_{tot}
- (4) Escape-plane inclination i_e , or nodal longitude of the escape plane η_N (see sketch (b))
- (5) Encounter-plane inclination i_m , or nodal longitude of the planetocentric encounter plane η_{NP}
- (6) Type of trip, direct or nodal (In a direct trip the vehicle travels in one plane during the heliocentric segment of its flight defined by the departure and encounter transition points on the respective spheres of influence (sketch (a)). In a nodal trip, two planes are involved during the heliocentric segment of the trip. The vehicle travels in the



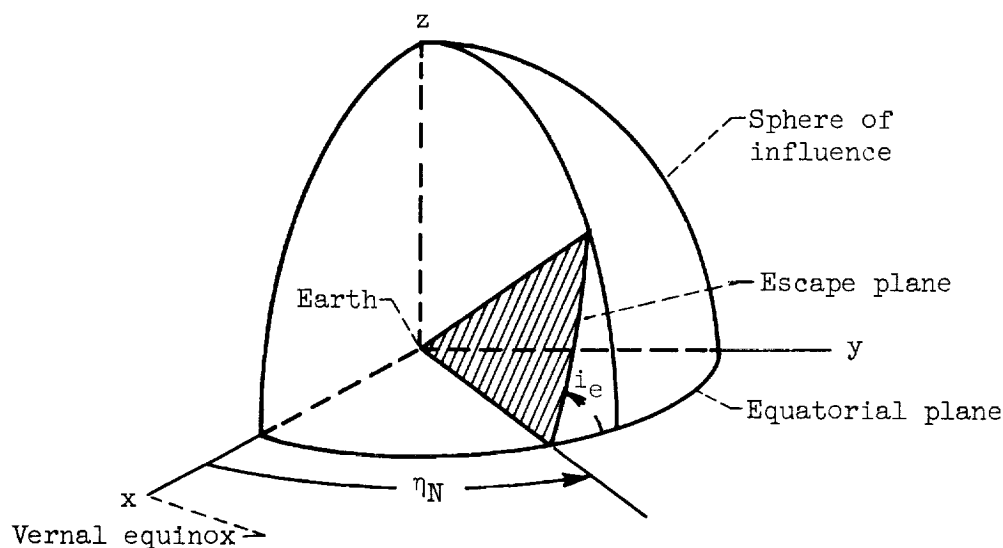
General geometry of model



Segmentation of trajectory

(a) Typical three-dimensional trajectory to Mars.

plane of the ecliptic until one of the two end points of the line of intersection of Mars' orbital plane and the ecliptic plane is reached. (This line is called the nodal line, while the points are called ascending node and descending node.) Then a ΔV is imparted such that the vehicle completes the remainder of the heliocentric segment in Mars' orbital plane.)



(b) Escape-plane orientation.

- (7) Type of parking orbit at Earth, direct (counterclockwise as seen from north equatorial pole) or retrograde (clockwise)
- (8) Type of parking orbit at destination planet, direct (counterclockwise as seen from north pole of Mars' orbital plane) or retrograde

From a typical calculation, the following information is obtained:

- (1) ΔV to depart from a given circular parking orbit
- (2) ΔV to establish a circular orbit on encounter at the destination planet
- (3) Orbital elements of the three required trajectory segments, that is, escape hyperbola, heliocentric segment, and the encounter hyperbola
- (4) Coast time on each trajectory segment
- (5) Perigee injection and perigee arrival coordinates

An iterative calculation is required to obtain a solution for a given set of inputs. An acceptable solution is achieved when two successive sets of coordinates for the escape and encounter transition points (located at Earth and the destination planets' spheres of influence, respectively) agree to within an arbitrary value of tolerance. The departure transition point connects the escape hyperbola and the heliocentric trajectory segment. The encounter transition point connects the heliocentric trajectory segment and the encounter hyperbola. For a tolerance of 10 miles (8.7 Int. naut. miles), the time required for a typical calculation is 5 seconds.

RESULTS AND DISCUSSION

This section is divided into three major subdivisions. The first compares the accuracy of the results obtained using the sphere-of-influence method and n-body calculations. The second discusses the effects of variation of geocentric and planetocentric parameters on the magnitude of the injection and arrival velocities and on the coordinates of the required injection and arrival perigee points for a 300-day mission from perigee at Earth to perigee at Mars. The third section presents interrelations among such overall mission parameters as trip time, heliocentric transfer plane inclination, orbit-to-orbit ΔV requirements, arrival communication distance, departure date, and synodic period of departure. The ΔV and communication distance requirements are compared with the circular-coplanar data of reference 6.

Evaluation of Method of Analysis

In order to illustrate the accuracy of the sphere-of-influence method, two typical trips were investigated. The results obtained are compared with those of n-body precision calculations. Included in the

precision calculations were the perturbing effects of the following bodies: Sun, Earth, Mars, Saturn, Jupiter, and the Moon. The Earth's oblateness was also included.

Table I indicates differences between the sphere of influence and the initial n-body escape hyperbola orbit and ΔV requirements to be small. All parameters for the 150-day trip agree to within 1 percent. Most parameters for the 300-day trip agree to within 3 percent. The negative signs in the percent difference column indicate the sphere-of-influence values to be less than those for the n-body calculations. The close agreement suggests that results from the sphere-of-influence method can be used advantageously as initial injection conditions for n-body precision calculations and for studying the effects of planet-centered trajectory segments on an overall interplanetary trip. The small velocity errors indicate two-body impulsive ΔV to be a reliable indication of propulsion requirements for use in high-thrust mission analyses.

Figure 1 indicates the positions of the vehicle relative to Earth and Mars for the 150- and 300-day trips, respectively. These typical trips illustrate the effect of trip time on the accuracy of the method of calculation. The path of the vehicle for the 300-day trip is more nearly "tangential" to the orbital paths of Earth and Mars on departure and arrival than for the 150-day trip (cf. figs. 1(a) and (b)). For the 300-day trip, the vehicle also has lower velocities with respect to Earth on injection and Mars on arrival (relative velocities) than for the 150-day trip. (Unless stated otherwise, all velocities will be considered as velocities of the vehicle with respect to the particular planet-centered segment of the trajectory being discussed.) Because of these two factors, vehicle velocity and path character, the perturbing effects of Earth and Mars are greater for the 300- than for the 150-day trip.

Effect of Planetocentric Trajectory Parameters

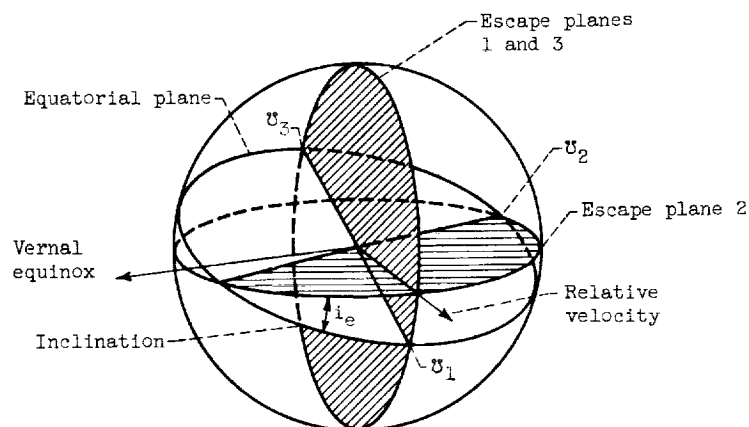
In planning interplanetary missions, a knowledge of the effects of planetocentric escape-plane inclination i_e and encounter-plane inclination i_m , injection time, and trajectory path angle α on injection and arrival coordinates and velocities is essential (see appendix B, sketch (n)). The effects of these parameters were investigated for a 300-day Earth-to-Mars trajectory. For this investigation of the planetocentric segments of the trajectory, the following conditions were fixed:

- (1) Radius of injection point, 1.1 Earth radii
- (2) Radius of arrival point, 1.1 Mars radii

The following parameters were assigned the values noted except when the parameters were varied to determine their effect on the 300-day trajectory:

Arbitrary injection time on Oct. 19, 1962	Universal time, 12 hr
Inclination of escape plane, i_e	90°
Injection trajectory angle, α_i	0°
Inclination of encounter plane, i_m	30° or 90°
Arrival trajectory angle, α_a	0°

Effect of escape-plane inclination. - The escape-plane inclination was varied over its possible range of values, which was found to be from 90° to 17.18° for this particular injection time and trip time (see sketch (c)). The velocity vector at the departure transition point (at the sphere of influence) remained nearly constant. The slight changes



	Escape plane		
	1	2	3
Plane of escape path			
Inclination, i_e , deg	90	17.18	90
Right ascension of descending node, U_N , deg	109.45	199.45	289.45
Relative velocity at sphere of influence			
Magnitude, miles/sec	1.98	1.98	1.98
Declination, deg	16.85	17.18	17.40
Right ascension, deg	109.45	109.45	109.45

(c) Range of possible escape-plane inclination from minimum to polar orbits for a given 300-day trip from Earth to Mars. Encounter-plane inclination, 90° ; arrival trajectory angle, 0° .

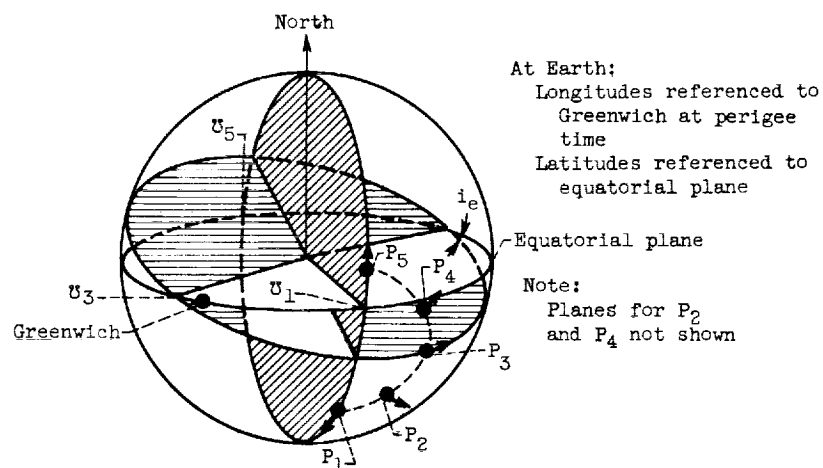
that did occur in the declination of the velocity vector were caused by the required changes in the heliocentric trajectory segment. These changes are required in order to match the coordinates of the geocentric trajectory segment (at the desired inclination) and the heliocentric segment at the transition point. Since the escape plane must contain the velocity vector at the transition point, a minimum escape-plane inclination exists for each injection time as explained in appendix B.

Sketch (d) shows the injection and arrival perigee coordinates for several escape-plane inclinations and an encounter-plane inclination of 30° . If the velocity vector at the departure transition point remained constant as the escape-plane inclination varied, the injection perigee points P_i would lie on a perfect small circle. (The section of a sphere made by a plane passing through the sphere but not its center is called a "small circle" of a sphere.) However, a quasi small circle results because of the slight variation in the declination of the velocity vector that accompanies a change in escape-plane inclination (see sketch (c)). If retrograde escape paths had been included, a complete quasi small circle would be shown on sketch (d).

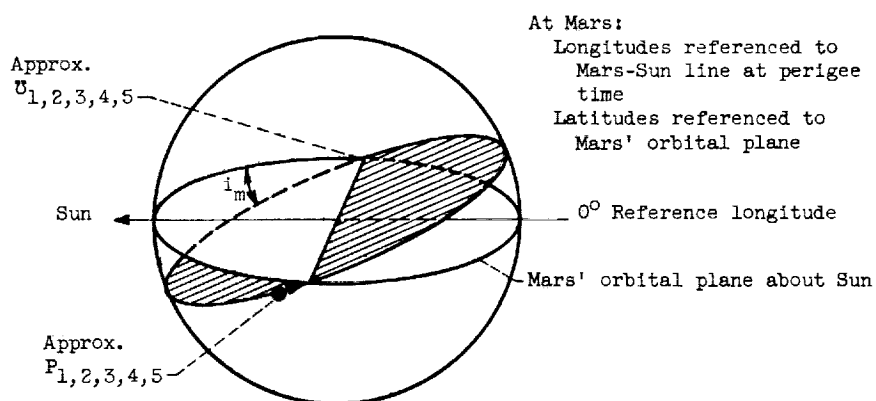
Variations of the geocentric orbit parameters are shown in figure 2 for the range of escape-plane inclinations investigated. Considering only direct motion of the vehicle, the declination λ_p of the perigee injection points varies from -48.3° to $+14.0^\circ$. The longitude ϕ_e of the perigee injection points varies from 84.5° E to 117.5° E. The magnitude of the injection velocity was found to be practically independent of escape-plane inclination. The azimuth of the injection velocity η_z varied from 0° to 180° . Increasing the encounter-plane inclination from 30° to 90° resulted in only slight changes in the geocentric orbit parameters, as shown in figure 2.

For the range of escape-plane inclinations (90° to 17.3°) investigated, only minor variations in the Mars-centered orbit parameters resulted, as shown in sketch (d) and figure 3. The coordinates of the arrival perigee points remained almost constant. The longitude and latitude varied by 0.21° and 0.5° , respectively. The arrival velocity varied by only 0.0023 mile per second.

Since the injection and arrival velocities are essentially independent of escape-plane inclination as determined by the present method, the mission ΔV is also independent of this parameter. Thus, an inclination can be selected to favor some mission requirement such as the use of available tracking stations or the avoidance of the intense regions of the Van Allen belts. The plane of the parking orbit at Earth would be selected to coincide with the selected escape plane.



Escape-orbit perigee	P_1	P_2	P_3	P_4	P_5
Inclination of plane, i_e , deg	90	30	17.3	30	90
Longitude of descending node, η_{NG}	84.5 E	51 E	358 E	300 E	265 E
Longitude of perigee, ϕ_e	84.5 E	116.5 E	117.5 E	113.5 E	84.5 E
Declination of perigee, λ_P	-48.3	-27.5	-15	-2.3	+14
Azimuth at perigee, η_Z	180	104.0	81.5	60	0



Encounter-orbit perigee	P_1	P_2	P_3	P_4	P_5
Inclination of plane, i_m , deg	30	30	30	30	30
Longitude of descending node, η_{NP}	64.85 E	64.60 E	64.41 E	64.21 E	63.82 E
Longitude of perigee, ϕ_m	236.87 E	236.85 E	236.83 E	236.78 E	236.66 E
Latitude of perigee, λ_{MP}	4.60 S	4.44 S	4.36 S	4.28 S	4.10 S
Azimuth at perigee, η_{ZF}	60.32	60.30	60.29	60.28	60.26

(d) Departure and arrival perigee coordinates and path azimuths for 300-day trip from Earth to Mars with departure from perigee at 1.1 Earth radii on October 19, 1962 (Greenwich noon) and arrival at perigee at 1.1 Mars radii.

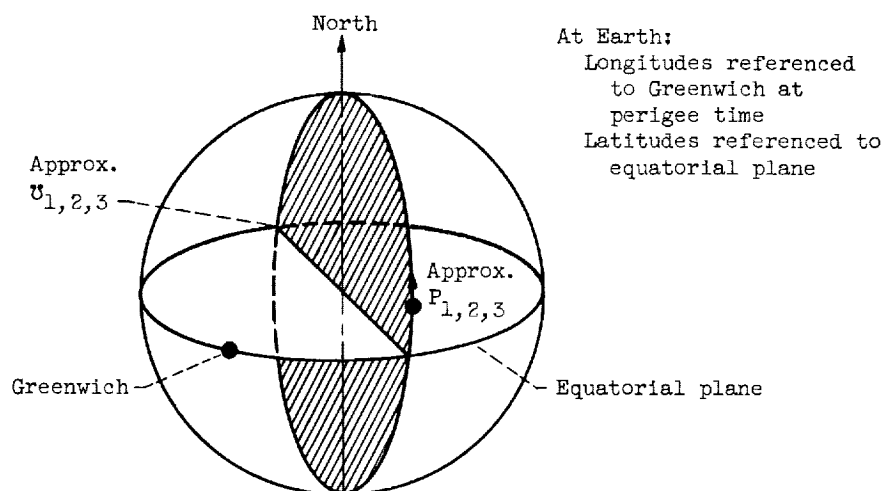
Effect of encounter-plane inclination. - The encounter-plane inclination was varied over its possible range to find its effects on the 300-day trajectory. For this portion of the analysis, the escape-plane inclination was fixed at 90° . The coordinates of the injection point and the injection velocity are practically independent of encounter-plane inclination (see sketch (e)). The latitude of the velocity vector at the arrival transition radius was found to be nearly constant for the range of possible encounter-plane inclinations. The slight changes that did occur were caused by required changes in the heliocentric trajectory segment. These changes were required in order to match the coordinates of the heliocentric trajectory segment and the encounter trajectory segment (for the desired inclination) at the encounter transition point.

For the possible range of encounter-plane inclinations the arrival perigee points formed a quasi small circle (see sketch (e)). A quasi small circle rather than a perfect small circle resulted again because of slight variations in the latitude of the velocity vector at the encounter transition point. Since the arrival points are perigee points of the respective encounter hyperbolas, the trajectory angle is 0° . If retrograde encounter paths had been included, a complete quasi small circle would be shown in sketch (e).

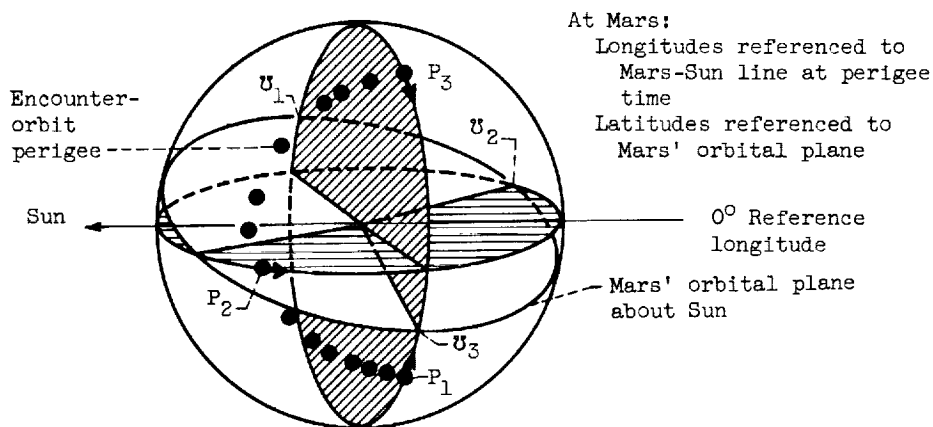
The effects on the planetocentric parameters of varying the encounter-plane inclination are shown in figure 4. For each arrival point, the magnitude of the arrival velocity was found to remain almost constant. The latitude of the arrival perigee points λ_{MP} varied from 31° S to 71° N of Mars' orbital plane. The longitude (ϕ_m , referenced to the Mars-Sun line at time of perigee) varied from 227° to 282° .

These results can be related to the orbit-to-orbit mission discussed in the previous section. Because the injection and arrival velocities are practically independent of encounter-plane inclination, the mission ΔV will be independent of this parameter provided the plane of the desired parking orbit at Mars is coincident with the selected encounter plane. Thus, the inclination of the encounter plane can be selected to favor a particular mission requirement. For example, an inclination might be selected to assure complete photographic coverage of Mars.

Effect of injection trajectory angle. - The effect of injection trajectory angle α_1 at 1.1 Earth radii on the departure and encounter transition point coordinates is presented in figures 5 and 6. The injection trajectory angle was varied by varying the perigee radius of the escape hyperbola. Therefore, in place of injection trajectory angle, the curves of figures 5 and 6 could have been labeled with the corresponding perigee radii. For a fixed escape-plane inclination, a 60° change in injection trajectory angle results in, at most, an 0.8° change



Escape-orbit perigee	P ₁	P ₂	P ₃
Inclination of plane, i_e , deg	90	90	90
Longitude of descending node, η_{NG} , deg	264.64 E	264.44 E	264.44 E
Longitude of perigee, ϕ_e , deg	84.64 E	84.44 E	84.44 E
Declination of perigee, λ_p , deg	+13.92	+13.97	+14.04
Azimuth at perigee, η_z , deg	0	0	0
Injection velocity, V_1	6.88	6.88	6.88



Encounter-orbit perigee	P ₁	P ₂	P ₃
Inclination of plane, i_m , deg	90	19.3	90
Longitude of descending node, η_{NP} , deg	101 E	10 E	281 E
Longitude of perigee, ϕ_m , deg	282 E	230 E	281 E
Latitude of perigee, λ_{MP} , deg	31 S	12 N	71 N
Azimuth at perigee, η_{zP} , deg	0	75.3	180

(e) Departure and arrival perigee coordinates and path azimuths for 300-day trip from Earth to Mars with departure from perigee at 1.1 Earth radii on October 19, 1962 (Greenwich noon) and arrival at perigee at 1.1 Mars radii.

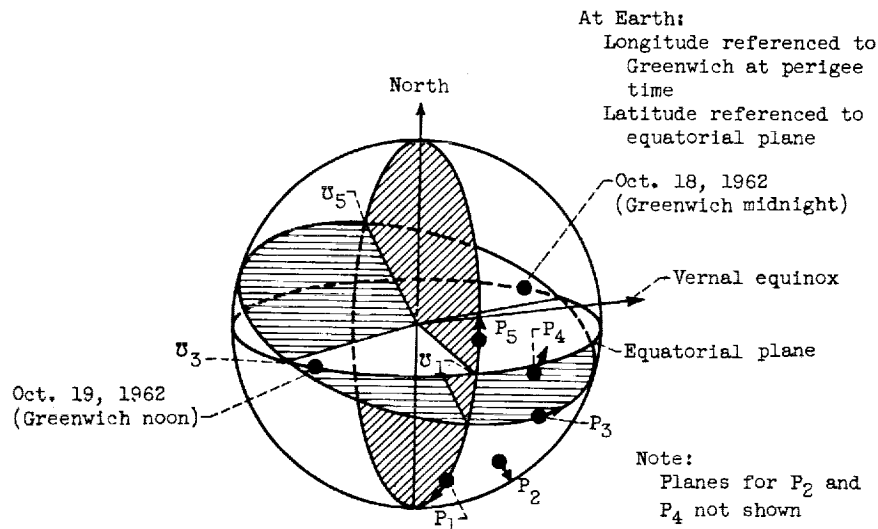
in either of the path coordinates at the Earth's sphere of influence (fig. 5) and an 0.025° change in longitude at Mars' sphere of influence (fig. 6). At both spheres of influence, the size of the quasi small circle shrinks as injection trajectory angle increases.

As the injection trajectory angle is increased, the velocity at the departure transition point remains essentially constant. Since the total energy of the escape hyperbola remains constant, the change in magnitude of the injection velocity for the range of conditions shown in figures 5 and 6 is only 0.001 mile per second. The arrival velocity varied by less than 0.0005 mile per second. Thus, both injection velocity and arrival velocity are nearly independent of injection trajectory angle. For a ground launch, the injection trajectory angle might be selected to favor some booster trajectory requirement. However, injection trajectory angles other than approximately 0° increase the booster propellant consumption because of greater gravity losses.

For circular orbit departures, injection trajectory angles other than 0° have a marked influence on the injection velocity increment. Figure 7 indicates the injection velocity increment associated with injection trajectory angles from 0° to 60° for a 300-day circular orbit-to-orbit mission. The velocity increment required at Earth ranged from 2.2 miles per second for a 0° injection trajectory angle to 6.1 miles per second for a 60° angle. Therefore, for circular-orbit departures, a 0° injection trajectory angle would be selected to minimize the velocity-increment requirement.

Effect of arrival trajectory angle. - The effect of arrival trajectory angle α_a on the coordinates of the transition point at Mars' sphere of influence is shown in figure 8. For a fixed value of encounter-plane inclination, the maximum change in longitude of the transition points is less than 0.4° . For the range of arrival trajectory angles and encounter-plane inclinations shown in figure 8, the variation in arrival velocity is 0.001 mile per second, and the variation in injection velocity is 0.0004 mile per second. Thus injection and arrival velocities are almost independent of arrival trajectory angle.

Effect of departure time. - Sketch (f) indicates the escape hyperbola path parameters for two 300-day trips to Mars. The departure times for these two trips differ by 12 hours. During this time the Earth rotates approximately 180.5° about its spin axis and revolves 0.5° in its orbit around the Sun. The values in the P_2 columns are representative of the changes that occur during a 12-hour period. The perigee coordinates, right ascension and declination, remain almost constant. Variations of 0.5° and 0.1° , respectively, were obtained. Injection velocity remains constant and its azimuth changes only 1° . The longitude of



Perigee injection - Oct. 18, 1962 (Greenwich midnight)					
Escape-orbit perigee	P_1	P_2	P_3	P_4	P_5
Inclination of plane, i_e , deg	90	30	17	30	90
Longitude of descending node, η_{NG}	266 E	234 E	176 E	118 E	86 E
Longitude of perigee, ϕ_e	266 E	298 E	298.5 E	294 E	266 E
Declination of perigee, λ_p	-48	-27.6	-14.4	-2	+14
Azimuth at perigee, η_Z	180	103.5	82	60	0
Right ascension of perigee, η_p	289.8 E	320.9 E	321.7 E	317.3 E	289.8 E
Injection velocity, V_i	6.88	6.88	6.88	6.88	6.88
Perigee injection - Oct. 19, 1962 (Greenwich noon)					
Inclination of plane, i_e , deg	90	30	17.5	30	90
Longitude of descending node, η_{NG}	84 E	51 E	360 E	298 E	265 E
Longitude of perigee, ϕ_e	84 E	115.8 E	117 E	113.5 E	84 E
Declination of perigee, λ_p	-48	-27.5	-15	-2.3	+14
Azimuth at perigee, η_Z	180	104.5	81	59.5	0
Right ascension of perigee, η_p	289.4 E	320.4 E	321.4 E	317.0 E	289.4 E
Injection velocity, V_i	6.88	6.88	6.88	6.88	6.88

(f) Departure perigee coordinates and path azimuth for 300-day trip from Earth to Mars with departure from perigee at 1.1 Earth radii on October 18, 1962 (Greenwich midnight) and October 19, 1962 (Greenwich noon) and arrival at perigee at 1.1 Mars radii. Inclination of planetocentric encounter plane, 90° .

perigee (ϕ_e , referred to Greenwich meridian at time of perigee injection) changes by 182.2° mostly because of the Earth's rotation.

The relations among a number of the trajectory variables are shown in figures 9 to 11 for a span in departure time of 1 day. For a constant escape-plane inclination, the right ascension and declination of the departure transition points vary by only 0.7° or less as shown in figure 9. Similarly, the inertial coordinates of the perigee injection points (right ascension and declination) vary only slightly for the same 1-day period (fig. 10). Figure 11 shows the relations among the following geocentric orbit parameters: departure time, escape-plane inclination, longitude of the descending node of the escape plane, the declination and longitude of the injection point, and the azimuth of the injection velocity. Figure 11 indicates all longitudes with respect to the Greenwich meridian at the time of perigee injection. The declination of all possible perigee injection points for the mission varied from about $+13.5^\circ$ to -48.5° . This same range was obtained for a fixed departure time. The longitude of possible perigee injection points varied through 360° . The azimuth of the injection velocity varied from 0° to 180° .

The magnitude of both the injection and the arrival velocities at 1.1 planet radii varied only slightly for the 1-day span of injection time investigated. For the orbit-to-orbit mission, the dependence on matching of trajectory segments produced changes in mission ΔV of less than 0.1 percent. This means that once during each orbit of the vehicle around Earth injection could occur without a significant penalty in the ΔV requirement. For example, if the plane of the parking orbit was oriented correctly with respect to nodal longitude and inclined at 30° , injection could occur every time the vehicle was at a latitude of about 2.5° S of the equator during a span of about 1 day. For a ground launch of the 300-day trajectory, injection time could be selected to favor a particular launch site.

Thus, from the preceding investigation of the planetocentric portions of a 300-day Earth-to-Mars trajectory, the following remarks can be made. The magnitude of the injection and arrival velocities is affected only slightly by rather wide variations in a number of the trajectory variables: inclination of escape plane, inclination of encounter plane, injection trajectory angle, arrival trajectory angle, and injection time. The significance of this is that in many missions values of these parameters can be selected to favor specific mission requirements.

Effect of Overall Trajectory Parameters

Previous discussion has shown the orbit-to-orbit mission ΔV to be insensitive to planetocentric escape- and encounter-plane inclination.

Therefore, arbitrary values of inclination were assigned during the study of the heliocentric segment of the trajectory. This study considers the interrelation among the following parameters: heliocentric transfer-plane inclination, orbit-to-orbit mission ΔV , trip time, departure date, and arrival communication distance.

In order to shorten the computing time required of the 704 computer, the tolerance for an acceptable solution was relaxed. Relaxing the tolerance induced errors of 0.05 percent or less in the velocity requirements, 0.25 percent or less in the communication distance, and 0.1° or less in the transfer-plane inclination.

Effect of trip time and departure date. - Figure 12 indicates the variation of the heliocentric travel angle θ for trip times of 150, 225, and 300 days as a function of departure date. Because the angular velocity of Earth is greater than that of Mars, the travel angle for a given trip time decreases for later departure dates. The 225- and 300-day trips require a travel angle of 180° for departure dates of September 13, 1962 and November 19, 1962, respectively. Travel angles near 180° are of special interest in a three-dimensional analysis because of their effect on transfer-plane inclination and ΔV requirements.

Because the orbital plane of Mars is inclined with respect to the ecliptic plane (1.85°), the inclination of the heliocentric transfer plane increases rapidly for trips having travel angles near 180° (fig. 13). This increase in inclination is accompanied by an increase in the normal components of the vehicle's heliocentric departure and arrival velocities. Therefore, the orbit-to-orbit ΔV requirements also increase with inclination. When the ecliptic angle between Earth and Mars is 180° , a maximum value of ΔV occurs since an inclination of 90° is required of the transfer plane. The heliocentric travel angle in this case would be $180^\circ \pm \lambda_0$ (latitude of Mars with respect to the ecliptic plane). For each trip time shown in figure 14, a minimum ΔV requirement results by selecting a particular launch date.

In the region of 180° travel angle, a two-plane transfer can overcome the disadvantage of high ΔV required of a single-plane transfer. One type of two-plane transfer is a nodal transfer in which the space vehicle travels in the plane of the ecliptic until the line of the Martian nodes is encountered. At this point a ΔV is imparted to the vehicle such that its velocity vector is rotated from the ecliptic plane to the Martian plane. The remainder of the heliocentric trajectory is then completed in the Martian plane. For trips with travel angles near 180° , a nodal transfer results in a lower mission ΔV than a direct transfer (fig. 15). The mission ΔV for a nodal transfer includes the ΔV required to change planes at the line of nodes. Except for the trips requiring high single-plane inclinations, the ΔV requirements for single-plane transfers are less than those for nodal transfers.

Effect of synodic period. - If the planetary orbits were circular and coplanar, a trajectory study for one synodic period would be sufficient. However, because of the inclinations and eccentricities of the planetary orbits, some marked differences in ΔV and transmission distance requirements can result for trajectories having the same trip time and the same departure configuration angle ψ (the angle between Earth and Mars on date of departure measured in the plane of the ecliptic) but launched in different synodic periods. The effects of synodic period on ΔV requirements and arrival communication distance are shown in figures 16 to 18. (Circular-coplanar results are also shown and will be discussed in a later section.)

Orbit-to-orbit mission ΔV requirements for trips to Mars in 1962 and 1971 are shown in figures 16(a) and (b) for trip times of 150 and 300 days, respectively. The separation distances during the oppositions related to these years are approximately the maximum and minimum distances that can occur. The February 3, 1963 opposition distance is 61.8 million miles (53.7 million Int. naut. miles), while that of August 6, 1971 is 34.6 million miles (30.1 million Int. naut. miles). The orbit-to-orbit mission ΔV for the 150-day trip in 1962 is approximately 1 mile per second higher than that in 1971. However, the reverse is true for the 300-day trip indicated in figure 16(b).

The ΔV differences between the 1962 and 1971 data of figure 16 are due mainly to the eccentricities of the orbits of Earth (0.0167) and Mars (0.0934). Mars is about 26 million miles (22.6 million Int. naut. miles) farther from the Sun when at aphelion than when at perihelion. Its perihelion velocity is about 3 miles per second greater than its aphelion velocity.

The velocity increments required at Earth and Mars for a direct transfer are compared in figure 17 with those required for a nodal transfer. The velocity increments for a nodal-type transfer are not penalized by inclination since no plane change is required on departure or arrival. As indicated, the velocity increments required of a direct- and a nodal-type trip at the planets are approximately equal. Therefore, the effect of inclination of the transfer plane on the ΔV requirements for these direct trajectories is slight.

In addition to affecting the ΔV requirements, the eccentricities of the planetary orbits can cause significant variations in the transmission distance, or straight-line distance between Earth and Mars on date of arrival. The sketch in figure 18(b) shows typical transmission distances for 300-day trips in 1962 and 1971. Figure 18 indicates the variation of transmission distance with departure configuration angle. For the 150-day trips (fig. 18(a)), the transmission distance is 27 to 58 million miles (23.5 to 50.4 million Int. naut. miles) greater in 1962

than in 1971. For the 300-day trips (fig. 18(b)) the differences range from 60.4 to 77 million miles (52.5 to 66.9 million Int. naut. miles).

Comparison of three-dimensional and circular-coplanar results. - In reference 6 it is pointed out that the results of a circular-coplanar analysis of Earth-to-Mars trajectories are approximate and should be used only in the preliminary planning of missions. An indication of just how approximate circular-coplanar results are is shown in figures 16 to 18. For the 150-day trips of figure 16(a), the circular-coplanar mission ΔV values either fall between the 1962 and 1971 values or exceed the 1962 values by 4 percent (0.29 mile/sec) or less. For the 300-day trips of figure 16(b), the circular-coplanar values lie between the 1962 and 1971 values and exceed the 1962 values by 5.5 percent (0.20 mile/sec) or less.

Figure 17 shows the differences that exist between the circular-coplanar and three-dimensional ΔV values required at Earth and Mars for 150-day trips to Mars in 1962 and 1971. For both trips the differences at Mars were greater than those at Earth. At Mars the differences varied from 0 to 0.35 mile per second in 1962 and from 0.52 to 1.0 mile per second in 1971. These differences are caused by the eccentricities of the planets and, therefore, changes in radius, velocity, and trajectory angle. Because of Mars' larger eccentricity (0.093) compared with Earth's (0.0167), these parameters vary more for Mars in traveling from perihelion to aphelion. The circular-coplanar transmission distance values lie roughly midway between the 1962 and the 1971 values (fig. 18). The transmission distances for the 150- and 300-day trips were at the minimum 10 million (8.7 million Int. naut. miles) and 40 million miles (34.8 million Int. naut. miles) less, respectively, in 1971 and 22 million (19.1 million Int. naut. miles) and 19 million miles (16.5 million Int. naut. miles) more in 1962 than the circular-coplanar values. In view of these large discrepancies the use of circular-coplanar results is not recommended in specific Earth-to-Mars mission studies.

Choice of node on nodal trip. - On many nodal trajectories with heliocentric travel angles greater than 180° , the rotation of the velocity vector from the ecliptic to the Martian plane can be made at the first or second crossing of the line of nodes. An advantage exists in making the plane change at the node nearest the aphelion of the transfer ellipse in order to minimize the required velocity increment. This results in the minimum ΔV since the required increment is proportional to the vehicle's velocity ($\Delta V = 2V \cos \alpha \sin I_m/2$). A savings of 0.23 mile per second is realized for the 300-day trip by making the plane change near aphelion rather than perihelion, as shown in figure 19.

SUMMARY OF RESULTS

E-1451

Data from the three-dimensional, multiple two-body, sphere-of-influence method of analysis are of sufficient accuracy to permit the use of this procedure in investigating both the planetocentric and heliocentric segments of interplanetary trajectories. Results for specific flights of interest can also be used as initial conditions for n-body calculations.

For an interplanetary trip of fixed duration, the magnitudes of the injection and arrival velocities are affected only slightly during a span of 1 day in injection time by rather wide variations in a number of trajectory variables such as inclination of escape plane, inclination of encounter plane, injection trajectory angle, and arrival trajectory angle. While the inclinations of the escape and encounter planes may be varied without penalizing the mission velocity increment, injection and arrival trajectory angles other than zero increase the propulsion requirements for both parking-orbit and ground-launch departures. Thus, for many orbit-to-orbit missions, values of escape- and encounter-plane inclination can be selected to favor specific mission requirements, such as the use of available tracking stations or the avoidance of intense regions of the Van Allen belts.

For Earth-to-Mars trajectories, the synodic period has a pronounced effect on velocity-increment requirements and on the arrival communication distance. Approximately 1-mile-per-second additional increment in velocity and 27 to 58 million additional miles (23.5 to 50.4 million Int. naut. miles) in transmission distance are required for a 150-day trip in 1962 compared with one in 1971. For the same trip circular-coplanar velocity-increment results ranged from 0.9 mile per second too low in 1962 to 1.2 miles per second too high in 1971. Therefore, the use of circular-coplanar data is not recommended in specific Earth-to-Mars mission studies.

Lewis Research Center

National Aeronautics and Space Administration
Cleveland, Ohio, January 17, 1962

APPENDIX A

SYMBOLS

a	semimajor axis, miles
E	eccentric anomaly, deg
e	eccentricity
I	obliquity or inclination of equatorial plane with respect to the ecliptic plane, deg (see appendix B, sketch (i))
I_m	inclination of Martian orbital plane with respect to ecliptic plane, deg (see appendix B, sketch (r))
i_e	inclination of geocentric escape plane with respect to equatorial plane, deg
i_m	inclination of planetocentric encounter plane with respect to Martian orbital plane, deg
m	miss distance, mean anomaly, or mass (see appendix B, sketch (j))
n	mean orbital motion, deg/day
P	period of planet, days
P_l	perigee locations ($l = 1, 2, 3, \dots$)
p	semilatus rectum, miles
R	heliocentric radius, miles
r	planetocentric radius
T	time of perihelion passage
T_{tot}	trip time starting from orbit about Earth and ending in orbit about destination planet, days
T_{1-2}	trip time from departure transition point to encounter transition point
t	time, days
V	velocity, miles/sec

E-1451

v	true anomaly, deg (see appendix B, sketch (n))
x^*	heliocentric x-axis displacement of encounter transition point measured in Mars-ecliptic ascending node coordinate system, miles (see appendix B, sketch (r))
y^*	y-axis displacement; otherwise same as x^*
z^*	z-axis displacement; otherwise same as x^*
α	trajectory angle, or angle between velocity vector and local horizontal, deg (see appendix B, sketch (n))
β	angular displacement of radial component of vehicle's relative velocity from total velocity vector at sphere-of-influence radius, deg (see appendix B, sketch (j))
Γ	celestial latitude with respect to ecliptic plane, deg (see appendix B, sketch (p))
γ	angle measured in Martian orbital plane from Mars-ecliptic ascending node to Mars at time t , deg (see appendix B, sketch (q))
δ	z-axis, otherwise same as ξ
δ'	z-axis, otherwise same as ξ'
ξ	x-axis displacement of departure transition point in vernal equinox - equatorial coordinate system, miles (see appendix B, sketch (g))
ξ'	x-axis displacement of departure transition point in nominal departure ecliptic coordinate
η_N	right ascension of equatorial - escape-plane nodal line, deg (see appendix B, sketch (l))
η_{NG}	longitude of descending node of escape-orbit plane with equatorial plane measured east from Greenwich meridian at time of perigee injection, deg
η_{NP}	longitude of descending node of plane of encounter orbit with Mars' orbital plane measured from Mars-Sun line at time of perigee arrival, deg
η_P	right ascension of perigee injection point for desired perigee radius

$\eta_{Q,1}$	equatorial longitude of transition point measured from escape plane - equatorial node, deg (see appendix B, sketch (m))
$\eta_{Q,2}$	longitude of transition point measured in escape plane from escape plane - equatorial node, deg (see appendix B, sketch (m))
$\eta_{R,1}$	equatorial longitude of zero perigee transition point measured from escape plane - equatorial node, deg (see appendix B, sketch (l))
$\eta_{R,2}$	longitude of zero perigee transition point measured in escape plane from escape plane - equatorial node, deg (see appendix B, sketch (l))
η_T	right ascension of transition point for specified perigee, deg (see appendix B, sketch (m))
η_{TP}	longitude of vehicle transition point at destination planet's sphere of influence measured counterclockwise from planet-Sun line on date of arrival at sphere of influence, deg
η_{VE}	longitude of positive x'-axis of nominal departure coordinate system measured eastward from vernal equinox, deg (see appendix B, sketch (i))
η_Z	azimuth of injection velocity on departure from 1.1 Earth radii measured clockwise from north equatorial pole, deg
η_{ZP}	azimuth of arrival velocity vector at encounter perigee measured clockwise from Mars' north orbital pole, deg
η_O	right ascension of zero perigee transition point, deg (see appendix B, sketch (l))
θ	heliocentric travel angle measured in transfer plane from departure transition point to encounter transition point, deg (see appendix B, sketch (r))
λ	geocentric latitude with respect to equatorial plane, deg
λ_{MP}	planetocentric latitude of perigee of encounter orbit with respect to Mars' orbital plane, deg
λ_{MT}	planetocentric latitude of transition point of encounter orbit with respect to Mars' orbital plane, deg

E-1451

μ	x-axis displacement of space vehicle encounter transition point in nominal arrival coordinate system, miles (see appendix B, sketch (q)), or force constant
ν	y-axis; otherwise same as μ
ξ	z-axis; otherwise same as μ
ρ	R_2 / R_1
σ	y-axis; otherwise same as ξ
σ'	y-axis; otherwise same as ξ'
τ	inclination of heliocentric transfer plane with respect to ecliptic plane, deg (see appendix B, sketch (r))
ϕ_e	longitude of perigee of escape hyperbola measured in equatorial plane counterclockwise from Greenwich meridian at time of perigee, deg
ϕ_m	longitude of perigee of encounter hyperbola measured in Martian orbital plane counterclockwise from positive x-axis or planet-Sun line at time of encounter perigee, deg
ψ	heliocentric ecliptic angle from Earth to Mars at time of injection, deg
ω	orbital longitude of perigee measured counterclockwise from escape plane - equatorial ascending node, deg (see appendix B, sketch (o))
ω_b	angle measured in ecliptic from departure transition point to Mars-ecliptic ascending node, deg (see appendix B, sketch (p))
ω_c	angle measured in ecliptic from Mars-ecliptic ascending node to encounter transition point projected, deg (see appendix B, sketch (r))
ω_D	angle measured in ecliptic from Earth to Mars-ecliptic ascending node, deg (see appendix B, sketch (p))
ω_e	angle measured in ecliptic from Earth to departure transition point projected, deg (see appendix B, sketch (p))
Ω	Mars ascending ecliptic node (see appendix B, sketch (p))

u_N locations of escape- or encounter-plane's descending node ($N = 1, 2, 3, \dots$)

Subscripts:

a arrival at 1.1 Mars radii

C,P circular velocity at desired radius

D perigee of encounter hyperbola at 1.1 Mars radii

E escape hyperbola

i injection at 1.1 Earth radii

INF sphere of influence

N normal component

NX x-axis component in nominal departure ecliptic coordinate system

NY y-axis, otherwise same as NX

NZ z-axis, otherwise same as NX

P perigee of escape hyperbola at 1.1 Earth radii

PL planet

R radial component

S Sun

T transition point

TX x-axis component in vernal equinox - equatorial coordinate system

TY y-axis, otherwise same as TX

TZ z-axis, otherwise same as TX

0 zero perigee or initial

1 departure transition point

2 encounter transition point

\oplus Earth

\circ Mars

APPENDIX B

CALCULATION PROCEDURE

Planet Position and Velocity

Before any of the geocentric or heliocentric requirements for a given interplanetary trip can be determined, Earth and the destination planet must be located. Kepler's equation is used in determining the orbital radius and velocity for Earth and the destination planet at time of injection and arrival, respectively. Orbital elements were chosen that would best fit the calculated positions of the planets with those indicated in references 7 and 8. The solution of Kepler's equation as given in reference 9 is presented in equations (B1) to (B7).

Kepler's equation

$$n(t - T) = m = E - e \sin E \quad (B1)$$

which is transcendental in E , is solved by iteration. The mean angular motion of the planet in its orbit is obtained from

$$n = \frac{114.592 \pi}{P} \quad (B2)$$

while the mean anomaly m is

$$m = n(t - T) \quad (B3)$$

An initial value of eccentric anomaly E_0 is obtained from the equation

$$E_0 = m + e \sin m + \frac{e^2}{2} \sin 2m \quad (B4)$$

The corresponding value of the mean anomaly can be obtained from Kepler's equation (B1):

$$m_0 = E_0 - e \sin E_0 \quad (B5)$$

A new value of E is obtained by applying a correction to E_0 :

$$\Delta E = \frac{m - m_0}{1 - e \cos E_0} \quad (B6)$$

Therefore,

$$E_1 = E_0 + \Delta E \quad (B7)$$

Equations (B5) to (B7) are iterated until an acceptably small difference, ΔE , is obtained. Knowing the eccentric anomaly, the true anomaly of the particular planet for the time specified is defined by

$$\cos v = \frac{\cos E - e}{1 - e \cos E} \quad (B8)$$

$$\sin v = \frac{\sqrt{1 - e^2} \sin E}{1 - e \cos E} \quad (B9)$$

The heliocentric radius for the position specified is

$$R = \frac{a(1 - e^2)}{1 + e \cos v} \quad (B10)$$

while the trajectory angle is determined from

$$\alpha = \tan^{-1} \left(\frac{e \sin v}{1 + e \cos v} \right) \quad (B11)$$

and the velocity from

$$v = \frac{\sqrt{\mu(2a - R)}}{aR} \quad (B12)$$

Geocentric Segment of Trajectory

Since expressions derived for either departure from Earth or encounter at Mars would be similar, the analysis herein will be confined to the departure or geocentric segment of the trajectory. The purpose of the geocentric analyses is to (1) define the escape hyperbola and (2) determine the coordinates of the starting point (perigee injection point) and the end point (transition point) of the geocentric escape hyperbola.

The following parameters are required for the geocentric portion of the calculation procedure:

- (1) Sphere-of-influence radius, r_{INF}
- (2) Perigee injection radius, r_p

- (3) Inclination of escape plane i_e or longitude of the nodal line η_N of escape plane
- (4) Components of vehicle's velocity relative to Earth at Earth's sphere of influence (V_{NX} , V_{NY} , V_{NZ}).

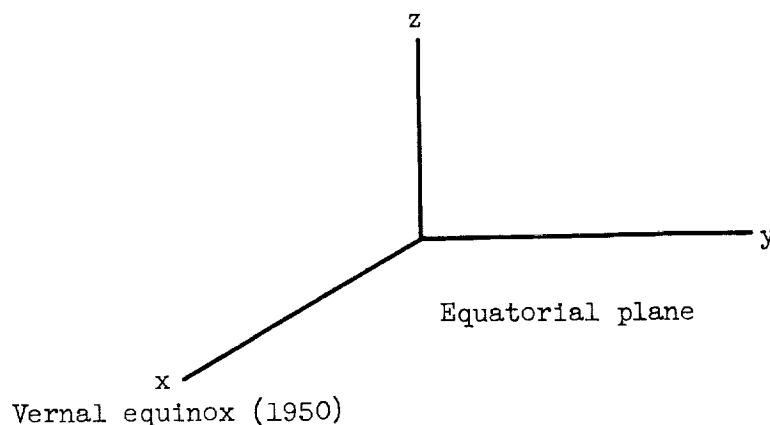
The first three are given, while the fourth is obtained from the heliocentric portion of the calculation procedure discussed later.

Sphere of influence. - The sphere of influence employed in this three-dimensional, two-body analysis serves as a boundary, inside of which the planet is considered as the central force while all other perturbing effects are neglected. The radius of this sphere is

$$r_{INF} = r_{PL} \left(\frac{m_{PL}}{m_S} \right)^{2/5} \quad (B13)$$

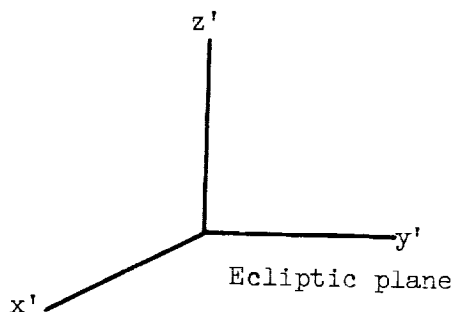
which for Earth is 575,000 miles (499,617.5 Int. naut. miles) and for Mars is 360,000 miles (312,823.0 Int. naut. miles). These values were chosen since they resulted in better initial values of the geocentric escape-orbit parameters for use in the precision calculation than were obtained using other radii (better in the sense that they resulted in a smaller miss distance at the destination planet than that of the desired encounter-orbit radius of $1.1 r_{PL}$).

Coordinate system. - In the analysis of the geocentric portion of the trajectory, a coordinate system was chosen having the equatorial plane as the x-y plane, the x-axis positive in the direction of the vernal equinox, the z-axis positive in the direction of the north equatorial pole, and the y-axis to complete the right-hand coordinate system as shown in sketch (g):



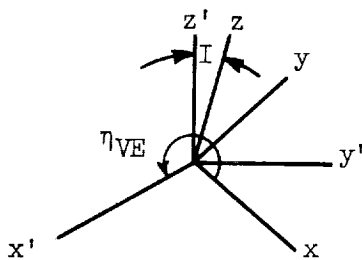
(g) Geocentric coordinate system.

From the heliocentric segment of the trajectory (discussed in a later section entitled "Determination of heliocentric travel angle") the components of the space vehicle's velocity relative to Earth at the sphere of influence are given with respect to the nominal departure coordinate system shown in sketch (h). In this system the x' -axis is the Earth-Sun



(h) Nominal departure system.

line at time of departure from the sphere of influence and is measured as positive in the direction away from the Sun, the z' -axis is positive in the direction of the north ecliptic pole, and the y' -axis completes the right-hand coordinate system. In order to obtain the x - y - z components of the relative velocity in the vernal equinox - equatorial system, two rotations are required as shown in sketch (i). The first



(i) Coordinate transformation.

rotation will determine the x - y - z components in the vernal equinox - ecliptic system. The second rotation will determine the x - y - z components in the vernal equinox - equatorial system. Combining these two rotations, the x - y - z components in the vernal equinox - equatorial system are

$$\left. \begin{aligned} V_{TX} &= V_{NX} \cos \eta_{VE} - V_{NY} \sin \eta_{VE} \\ V_{TY} &= (V_{NX} \sin \eta_{VE} + V_{NY} \cos \eta_{VE}) \cos I - V_{NZ} \sin I \\ V_{TZ} &= (V_{NX} \sin \eta_{VE} + V_{NY} \cos \eta_{VE}) \sin I + V_{NZ} \cos I \end{aligned} \right\} \quad (B14)$$

where I is the obliquity of the ecliptic plane and η_{VE} is the angle from the vernal equinox of 1950 eastward to the nominal x-axis.

Two points on the planetocentric conic will be of major importance in the resulting relations. These points are the perigee injection point, at a desired perigee radius, and the transition point at the sphere of influence where the vehicle's motion is considered to change from geocentric to heliocentric. The coordinates of the geocentric and heliocentric trajectory segments will be matched by means of iteration.

Determination of transition-point coordinates. - If initially a perigee radius of zero is assumed, the coordinates for the transition point can be written as

$$r_{INF}^2 = r_T^2 = X_T^2 + Y_T^2 + Z_T^2 \quad (B15)$$

Differentiating gives

$$r_T \dot{r}_T = X_T \dot{X}_T + Y_T \dot{Y}_T + Z_T \dot{Z}_T \quad (B16)$$

Also

$$V_T^2 = \dot{X}_T^2 + \dot{Y}_T^2 + \dot{Z}_T^2 \quad (B17)$$

But, since the perigee radius was stated as zero,

$$\dot{r}_T = V_T \quad (B18)$$

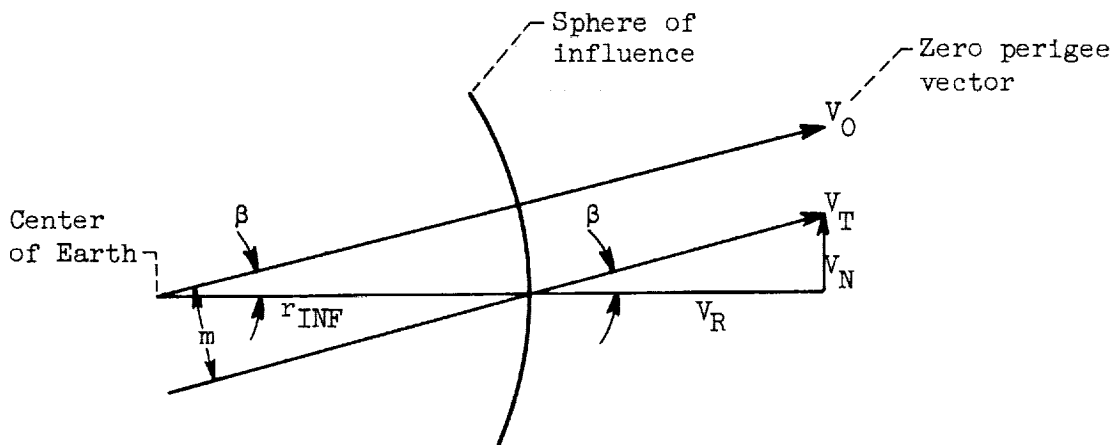
Therefore,

$$\frac{X_T \dot{X}_T}{r_T} + \frac{Y_T \dot{Y}_T}{r_T} + \frac{Z_T \dot{Z}_T}{r_T} = \frac{\dot{X}_T^2}{V_T} + \frac{\dot{Y}_T^2}{V_T} + \frac{\dot{Z}_T^2}{V_T}$$

or

$$\frac{X_T}{r_T} = \frac{\dot{X}_T}{V_T}, \quad \frac{Y_T}{r_T} = \frac{\dot{Y}_T}{V_T}, \quad \frac{Z_T}{r_T} = \frac{\dot{Z}_T}{V_T} \quad (B19)$$

For a perigee radius other than zero, the relative velocity vector V_T at the sphere of influence must be displaced by a miss distance m as seen in sketch (j). The relative velocity is defined as the velocity of the vehicle with respect to Earth.



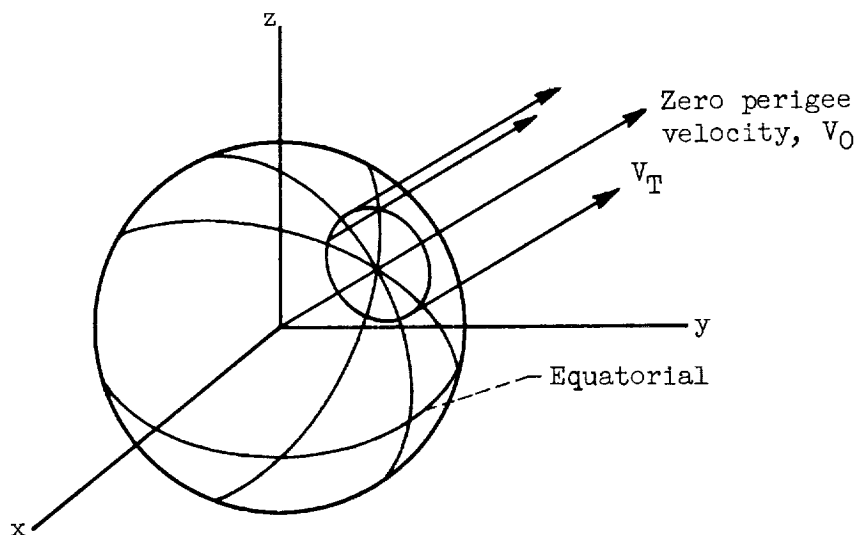
(j) Departure transition point.

From similar triangles

$$\frac{m}{r_{INF}} = \frac{V_N}{V_T} = \sin \beta \quad (B20)$$

Equal offset distances on either side of the zero perigee or all radial case result in identical hyperbolic orbits, except that their sense of rotation is either direct (counterclockwise) or retrograde (clockwise) as seen from the equatorial north pole. Therefore, for a fixed perigee radius two possible departure (or transition) points and, therefore, two possible perigee injection-point locations exist for this two-dimensional case.

As shown in sketch (k), the transition point for the case of the perigee radius equal to zero is contained by an infinite number of great-circle planes. Any particular great-circle plane passing through the zero perigee transition point has a resulting inclination with the equatorial, x-y plane, and a resulting position of the nodal line in the x-y plane. Therefore, by specifying either the inclination of the escape plane or the longitude of the nodal line together with the transition point for a perigee radius of zero defined by the zero perigee velocity vector, the plane of the escape hyperbola is defined.



(k) Departure transition points.

If V_T remained constant in magnitude and direction as the escape-plane inclination was varied, a true small circle of transition points would result as shown in sketch (k). However, in actual calculations the magnitude and orientation of V_T change slightly, resulting in a quasi small circle of transition points.

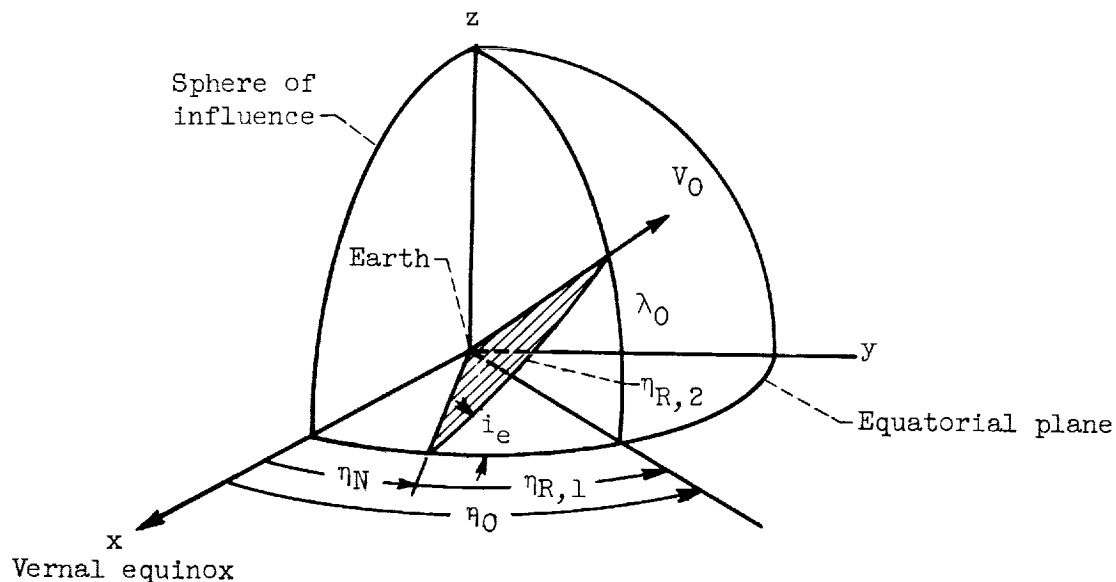
Sketch (l) shows one escape plane, determined by the zero perigee transition point and a given longitude of the nodal line η_N . The inclination of the escape plane is

$$i_e = \tan^{-1} \left(\frac{V_{TZ}}{V_{TY} \cos \eta_N - V_{TX} \sin \eta_N} \right) \quad (B21)$$

The longitude or right ascension of the transition point for a perigee radius of zero is defined by

$$\begin{aligned} \sin \eta_0 &= \frac{V_{TY}}{\sqrt{V_{TX}^2 + V_{TY}^2}} \\ \cos \eta_0 &= \frac{V_{TX}}{\sqrt{V_{TX}^2 + V_{TY}^2}} \end{aligned} \quad (B22)$$

since, as shown in equation (B19), the x-y-z coordinates for the zero perigee transition point are proportional to X_T , Y_T , and Z_T .



(1) Escape-plane nomenclature.

Therefore, from sketch (1)

$$\eta_{R,1} = \eta_0 - \eta_N \quad (B23)$$

and

$$\eta_{R,2} = \eta_{R,1} + \tan^{-1} \left[\frac{\tan \eta_{R,1} (1 - \cos i_e)}{\cos i_e + \tan^2 \eta_{R,1}} \right] \quad (B24)$$

For a perigee radius other than zero, the velocity vector must be displaced by β as shown in sketch (j) and equation (B20). In order to determine β for the perigee radius desired, the normal component of the velocity V_T must be known. This velocity component V_N is determined as follows:

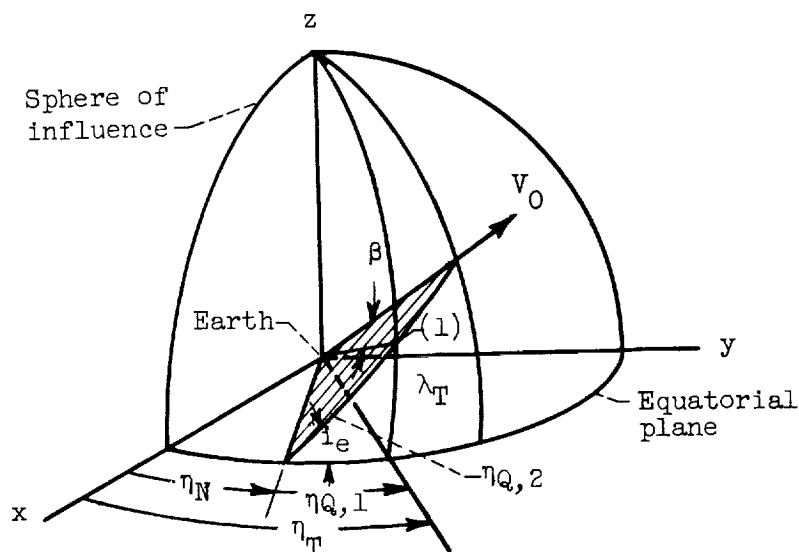
$$V_P^2 = V_T^2 + 2 \frac{\mu_\oplus}{r_P} \left(1 - \frac{r_P}{r_{INF}} \right) \quad (B25)$$

$$V_N = \frac{r_P V_P}{r_{INF}} \quad (B26)$$

From sketch (m) for direct motion of the space vehicle as seen from the north equatorial pole,

$$\eta_{Q,2} = \eta_{R,2} - \beta \quad (B27)$$

$$\eta_{Q,1} = \eta_{Q,2} - \tan^{-1} \left[\frac{\tan \eta_{Q,2} (1 - \cos i_e)}{1 + \cos i_e \tan^2 \eta_{Q,2}} \right] \quad (B28)$$



(m) Transition-point nomenclature.

The right ascension of the transition point is

$$\eta_T = \eta_N + \eta_{Q,1} \quad (B29)$$

and the declination is

$$\lambda_T = \tan^{-1} (\sin \eta_{Q,1} \tan i_e) \quad (B30)$$

The x-y-z or vernal equinox - equatorial coordinates of the transition point or ζ , σ , δ , respectively, are

$$\left. \begin{aligned} \zeta &= r_{\text{INF}} \cos \lambda_T \cos \eta_T \\ \sigma &= r_{\text{INF}} \cos \lambda_T \sin \eta_T \\ \delta &= r_{\text{INF}} \sin \lambda_T \end{aligned} \right\} \quad (\text{B31})$$

In the nominal $x'-y'-z'$ -coordinate system (sketch (h)), the coordinates of the transition point are

$$\left. \begin{aligned} \zeta' &= \zeta \cos \eta_{\text{VE}} + \sin \eta_{\text{VE}} (\sigma \cos I + \delta \sin I) \\ \sigma' &= -\zeta \sin \eta_{\text{VE}} + \cos \eta_{\text{VE}} (\sigma \cos I + \delta \sin I) \\ \delta' &= \delta \cos I - \sigma \sin I \end{aligned} \right\} \quad (\text{B32})$$

These coordinates are used in the heliocentric portion of the calculation procedure.

Parameters of escape hyperbola. - The parameters defining the required escape hyperbola are the eccentricity:

$$e_E = \frac{v_P^2 r_P}{\mu_\oplus} - 1.0 \quad (\text{B33})$$

the semilatus rectum:

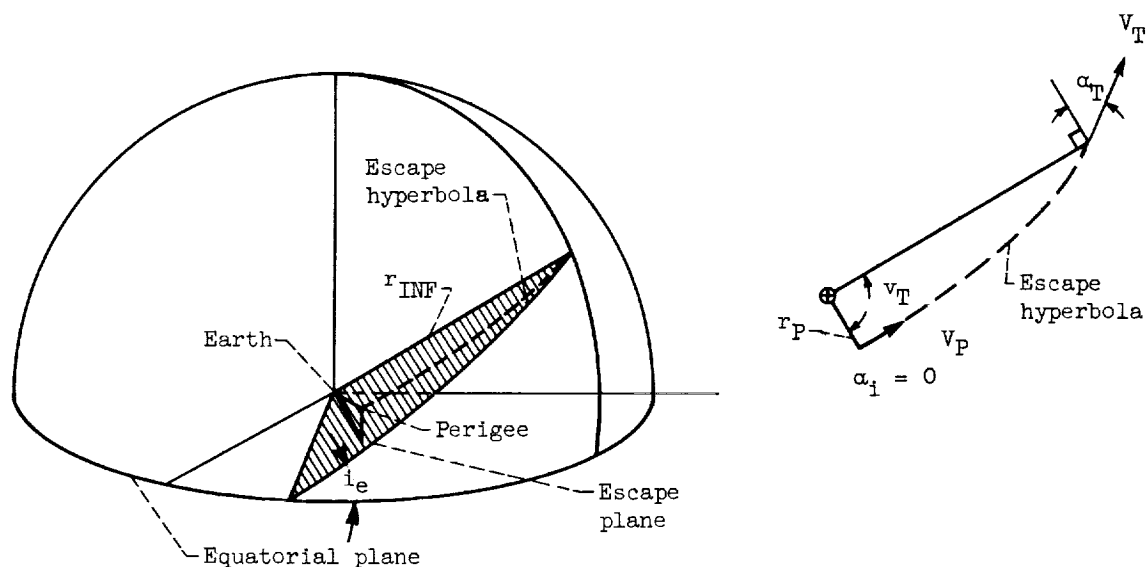
$$p_E = (e_E + 1.0)r_P \quad (\text{B34})$$

and the true anomaly of the departure transition point (sketch (n)):

$$\cos v_T = \frac{\frac{p_E}{r_{\text{INF}}} - 1.0}{e_E}$$

$$v_T = \tan^{-1} \left(\frac{\sqrt{1 - \cos^2 v_E}}{\cos v_E} \right) \quad (\text{B35})$$

E-1451

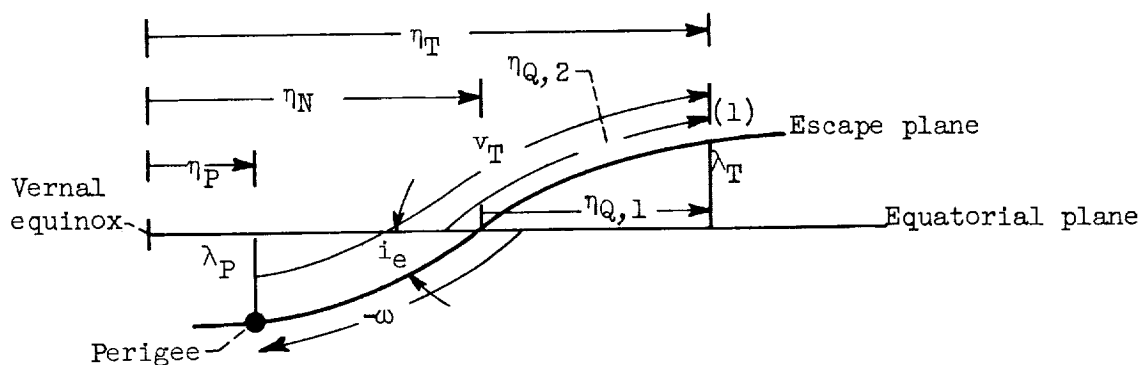


(n) Escape trajectory.

Determination of perigee injection-point coordinates. - Knowing the escape-plane inclination and the required true anomaly of the departure transition point (1), the right ascension and declination of the perigee injection point can be determined.

From sketch (o),

$$\omega = \eta_{Q,2} - v_T \quad (B36)$$



(o) Latitude plotted against longitude.

The geocentric latitude (declination) of the perigee injection point is defined by

$$\sin \lambda_P = \sin i_e \sin \omega \quad (B37)$$

$$\cos \lambda_P = \sqrt{1 - \sin^2 \lambda_P} \quad (B38)$$

Therefore,

$$\lambda_P = \tan^{-1} \left(\frac{\sin \lambda_P}{\cos \lambda_P} \right) \quad (B39)$$

The right ascension of the perigee injection point is

$$\eta_P = \eta_N + 2 \tan^{-1} \left[\frac{\sin \lambda_P}{\tan i_e (\cos \lambda_P + \cos \omega)} \right] \quad (B40)$$

Injection velocity increment. - For departure from a circular parking orbit at 1.1 Earth radii, the velocity increment required at perigee injection is

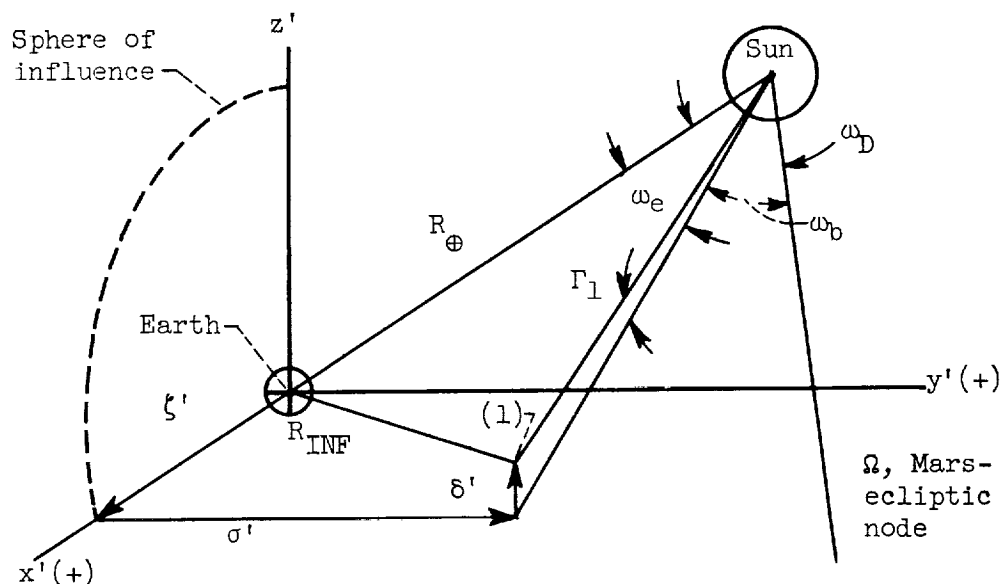
$$\Delta V_P = V_P - V_{C,P} \quad (B41)$$

Heliocentric Segment of Trajectory

Upon arrival at the Earth's sphere of influence, the vehicle's motion is assumed to change from geocentric to heliocentric. The heliocentric segment of the trajectory then starts at the Earth's sphere of influence and ends at Mars' sphere of influence. The purpose of this part of the calculation procedure is then to:

- (1) Determine the required heliocentric transfer conic connecting the departure transition point and the encounter transition point for a given trip time
- (2) Determine the required inclination of the transfer plane with respect to the plane of the ecliptic
- (3) Determine the heliocentric velocity of the vehicle at both the departure and the encounter transition points.

Determination of heliocentric travel angle. - On departure from the sphere of influence at Earth, the coordinates of the space vehicle ζ' , σ' , and δ' , shown in sketch (p), are given along with the heliocentric orbital radius of Earth obtained previously.



(p) Heliocentric coordinates of departure point.

From sketch (p),

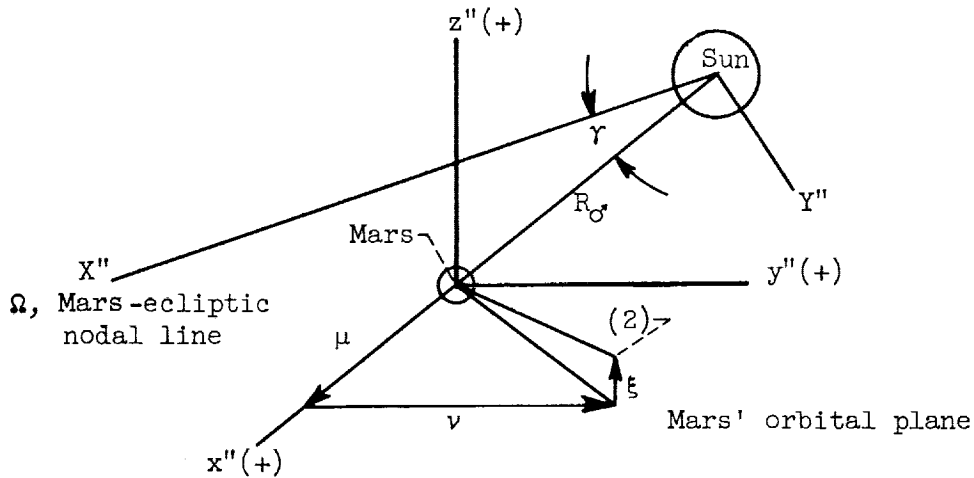
$$\omega_e = \tan^{-1} \left(\frac{\sigma'}{R_{\oplus} + \zeta'} \right) \quad (B42)$$

Given the angle from Earth's perihelion (1960) to Mars' ascending node, the angle ω_D can be determined knowing the true anomaly of Earth on date of departure. Therefore,

$$\omega_b = \omega_D - \omega_e \quad (B43)$$

From sketch (p)

$$\Gamma_1 = \tan^{-1} \left(\frac{\delta'}{\sqrt{(R_{\oplus} + \zeta')^2 + (\sigma')^2}} \right) \quad (B44)$$



(q) Heliocentric coordinates of arrival point.

Sketch (q) indicates the x'' - y'' - z'' coordinates of the space vehicle on arrival (point (2)) at Mars' sphere of influence in the nominal arrival coordinate system. This system has as its x'' -axis the Mars-Sun line on the date of arrival at Mars' sphere of influence. The z'' -axis is normal to Mars' orbital plane, and the y'' -axis completes the right-hand coordinate system.

The heliocentric (x - y - z) coordinates of point (2) referenced to the ascending node - ecliptic coordinate system (X'' - Y'' - Z'') are given in equations (B45). This coordinate system has as its x -axis the Mars-ecliptic nodal line. The z -axis is normal to the ecliptic plane.

$$\left. \begin{aligned} x^* &= (R_{\odot} + \mu) \cos \gamma - v \sin \gamma \\ y^* &= [(R_{\odot} + \mu) \sin \gamma + v \cos \gamma] \cos I_m - \xi \sin I_m \\ z^* &= [(R_{\odot} + \mu) \sin \gamma + v \cos \gamma] \sin I_m + \xi \cos I_m \end{aligned} \right\} \quad (B45)$$

where I_m is the inclination of Mars' orbital plane with respect to the plane of the ecliptic.

The heliocentric transfer plane is shown in sketch (r):



(r) Heliocentric trajectory.

The celestial latitude of point (2) is

$$\Gamma_2 = \tan^{-1} \left(\frac{z^*}{\sqrt{(x^*)^2 + (y^*)^2}} \right) \quad (\text{B46})$$

The angle labeled ω_c in sketch (r) is calculated from

$$\sin \omega_c = \frac{y^*}{\sqrt{(x^*)^2 + (y^*)^2}} \quad (B47)$$

$$\cos \omega_c = \frac{x^*}{\sqrt{(x^*)^2 + (y^*)^2}} \quad (B47)$$

From sketch (r)

$$\omega_{bc} = \omega_b + \omega_c \quad (\text{B48})$$

By spherical trigonometry

$$\sin Q = \tan \Gamma_1 / \tan \tau \quad (\text{B49})$$

$$\sin (\omega_{\text{pc}} + Q) = \tan \Gamma_2 / \tan \tau \quad (\text{B50})$$

By using equations (B49) and (B50), the following equation can be obtained for the inclination of the transfer plane with respect to the ecliptic:

$$\tau = \tan^{-1} \left[\left(\frac{\tan \Gamma_2 - \cos \omega_{bc} \tan \Gamma_1}{\sin \omega_{bc}} \right)^2 + \tan^2 \Gamma_1 \right]^{1/2} \quad (\text{B51})$$

By spherical trigonometry

$$Q_S = \tan^{-1} \left(\frac{\tan Q}{\cos \tau} \right) \quad (\text{B52})$$

The heliocentric angle from the transfer plane - ecliptic node to point (2) measured in the transfer plane is

$$\left. \begin{aligned} \sin (\theta + Q_S) &= \sin \Gamma_2 / \sin \tau \\ \cos (\theta + Q_S) &= \cos \Gamma_2 \cos (\omega_{bc} + Q) \end{aligned} \right\} \quad (\text{B53})$$

These angles are indicated in sketch (r). Therefore, the heliocentric travel angle from point (1) to (2) measured in the plane of the transfer plane θ can be obtained:

$$\theta = (\theta + Q_S) - Q_S \quad (\text{B54})$$

Parameters of transfer conic. - The heliocentric departure and arrival radii are

$$R_1 = \left[(R_{\oplus} + \zeta')^2 + (\sigma')^2 + (\delta')^2 \right]^{1/2} \quad (\text{B55})$$

$$R_2 = \left[(x^*)^2 + (y^*)^2 + (z^*)^2 \right]^{1/2} \quad (\text{B56})$$

With θ , R_1 , R_2 and the trip time $T_{1,2}$ from points (1) to (2), the heliocentric conic section can be determined by iteration.

The general expression for travel time on a conic referenced to perihelion is as follows:

$$T = \frac{p^{3/2}}{\mu^{1/2}} \int_0^v \frac{dv}{(1 + e \cos v)^2} \quad (\text{B57})$$

Integrating this general equation for time, the specific time equations for an ellipse, a parabola, and a hyperbola are obtained:

$e < 1.0$:

$$T = \frac{p^{3/2}}{\mu_S^{1/2}(1 - e^2)} \left\{ \frac{-e \sin v}{1 + e \cos v} + \frac{2}{\sqrt{1 - e^2}} \left[\tan^{-1} \frac{\sqrt{1 - e^2} \sin v}{(1 + e)(1 + \cos v)} \right] \right\} \quad (B58)$$

$e = 1.0$:

$$T = \frac{p^{3/2}}{3\mu_S^{1/2}} \sin v \left[\frac{2 + \cos v}{(1 + \cos v)^2} \right] \quad (B59)$$

$e > 1.0$:

$$T = \frac{p^{3/2}}{\mu_S^{1/2}(1 - e)^2} \left[\frac{-e \sin v}{1 + e \cos v} + \frac{1}{\sqrt{e^2 - 1}} \ln \left(\frac{e + \cos v + \sqrt{e^2 - 1} \sin v}{1 + e \cos v} \right) \right] \quad (B60)$$

Equations (B58), (B59), and (B60) are transcendental in v ; therefore, there is no direct solution for v . An iterative solution is required to determine v_1 and v_2 given $T_{1,2}$, θ , R_1 , and R_2 . Assuming a value of v_1 the eccentricity can be found from

$$e = \left| \frac{1 - \frac{R_2}{R_1}}{\frac{R_2}{R_1} \cos v_2 - \cos v_1} \right| \quad (B61)$$

where $v_2 = v_1 + \theta$.

The semilatus rectum of the conic is

$$p = R_1(1 + e \cos v_1) \quad (B62)$$

Thus, depending on the eccentricity, equations (B58) to (B62) are iterated until an acceptably small difference in the calculated trip time and the required trip time is obtained.

The semimajor axis is

$$a = \frac{p}{1 - e^2} \quad (\text{B63})$$

The departure and arrival heliocentric trajectory angles are

$$\alpha_1 = \tan^{-1} \frac{e \sin v_1}{1 + e \cos v_1} \quad (\text{B64})$$

and

$$\alpha_2 = \tan^{-1} \frac{e \sin v_2}{1 + e \cos v_2}$$

The departure and arrival heliocentric velocities are

$$V_1 = \sqrt{\frac{\mu_S(2a - R_1)}{aR_1}} \quad (\text{B65})$$

and

$$V_2^2 = V_1^2 - \frac{2\mu_S}{\rho R_1} (\rho - 1) \quad (\text{B66})$$

where $\rho = R_2/R_1$.

Vehicle velocity relative to Earth at departure transition point. -
The $X'-Y'-Z'$ components of the departure heliocentric velocity are

$$\left. \begin{aligned} V_{1,X} &= V_1 \cos(\alpha_1 - Q_S) \cos \tau \sin (Q - \omega_e) + V_1 \sin(\alpha_1 - Q_S) \cos (Q - \omega_e) \\ V_{1,Y} &= V_1 \cos(\alpha_1 - Q_S) \cos \tau \cos (Q - \omega_e) - V_1 \sin(\alpha_1 - Q_S) \sin (Q - \omega_e) \\ V_{1,Z} &= V_1 \cos (\alpha_1 - Q_S) \sin \tau \end{aligned} \right\} \quad (\text{B67})$$

The X' and Y' components of the Earth's velocity are

$$\left. \begin{aligned} V_{EX} &= V_{\oplus} \sin \alpha_{\oplus} \\ V_{EY} &= V_{\oplus} \cos \alpha_{\oplus} \end{aligned} \right\} \quad (B68)$$

Therefore, in the nominal departure coordinate system (sketch (p)) the X' - Y' - Z' components of the relative velocity at the departure transition point are

$$\left. \begin{aligned} V_{NX} &= V_{1,X} - V_{EX} \\ V_{NY} &= V_{1,Y} - V_{EY} \\ V_{NZ} &= V_{1,Z} \end{aligned} \right\} \quad (B69)$$

These components of the relative velocity are now used to determine a new set of departure transition point coordinates. This iterative procedure is used until an acceptably small difference in the transition point coordinates is obtained.

REFERENCES

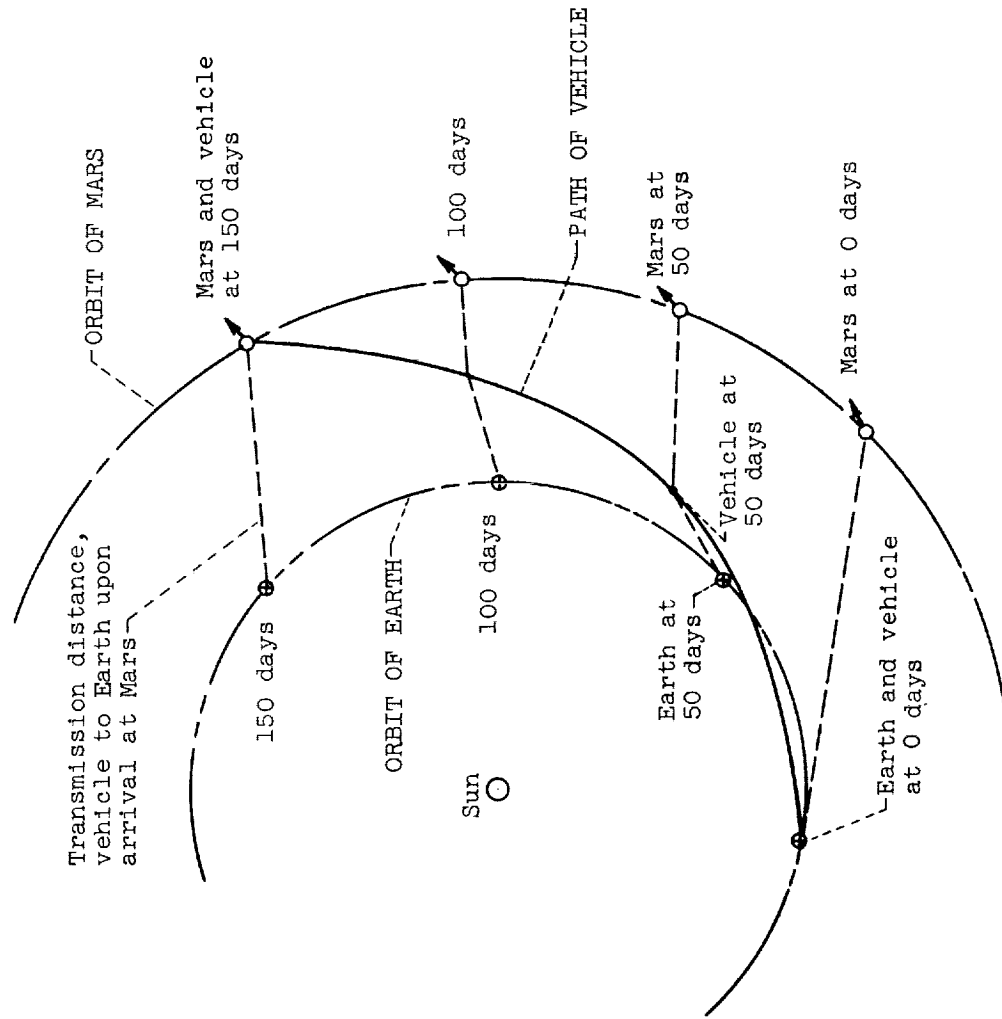
1. Karrenberg, Hans K., and Arthur, Paul D.: Interplanetary Ballistic Orbits. Preprint 870-59, Am. Rocket Soc., Inc., 1959.
2. Breakwell, John V., Gillespie, Rollin W., and Ross, Stanley: Researches in Interplanetary Transfer. Preprint 954-59, Am. Rocket Soc., Inc., 1959.
3. Mickelwait, A. B., Tompkins, E. H., Jr., and Park, R. A.: Three-Dimensional Interplanetary Ballistic Trajectories. Inst. Radio Eng. Trans. on Military Electronics, vol. MIL-3, no. 4, Oct. 1959, pp. 149-159.
4. Moeckel, W. E.: Departure Trajectories for Interplanetary Vehicles. NASA TN D-80, 1959.
5. Bossart, Karel J.: Techniques for Departure and Return in Interplanetary Flight. Paper presented at IAS 1958 Nat. Midwestern meeting, St. Louis (Mo.), May 14, 1958.
6. Dugan, James F., Jr.: Analysis of Trajectory Parameters for Probe and Round-Trip Missions to Mars. NASA TN D-281, 1960.

7. Clemence, G. M., and Wollard, Edgar W.: The American Ephemeris and Nautical Almanac for 1959. U.S. Govt. Printing Office, Wash., D.C., 1959.
8. H. M. Nautical Almanac Office: Planetary Coordinates for the Years 1960-1980. Her Majesty's Stationery Office (London), 1958.
9. Moulton, Forest Ray: An Introduction to Celestial Mechanics. Second revised ed., 1958.

TABLE I. - COMPARISON OF PARAMETERS OBTAINED FROM TWO-BODY TRAJECTORY CALCULATION WITH THOSE REQUIRED IN PRECISION (n-BODY) CALCULATION FOR TWO TRIPS TO MARS FROM PERIGEE AT 1.1 EARTH RADII TO PERIGEE AT 1.1 MARS RADII

[Constant-orbit elements were used to determine positions of planets.]

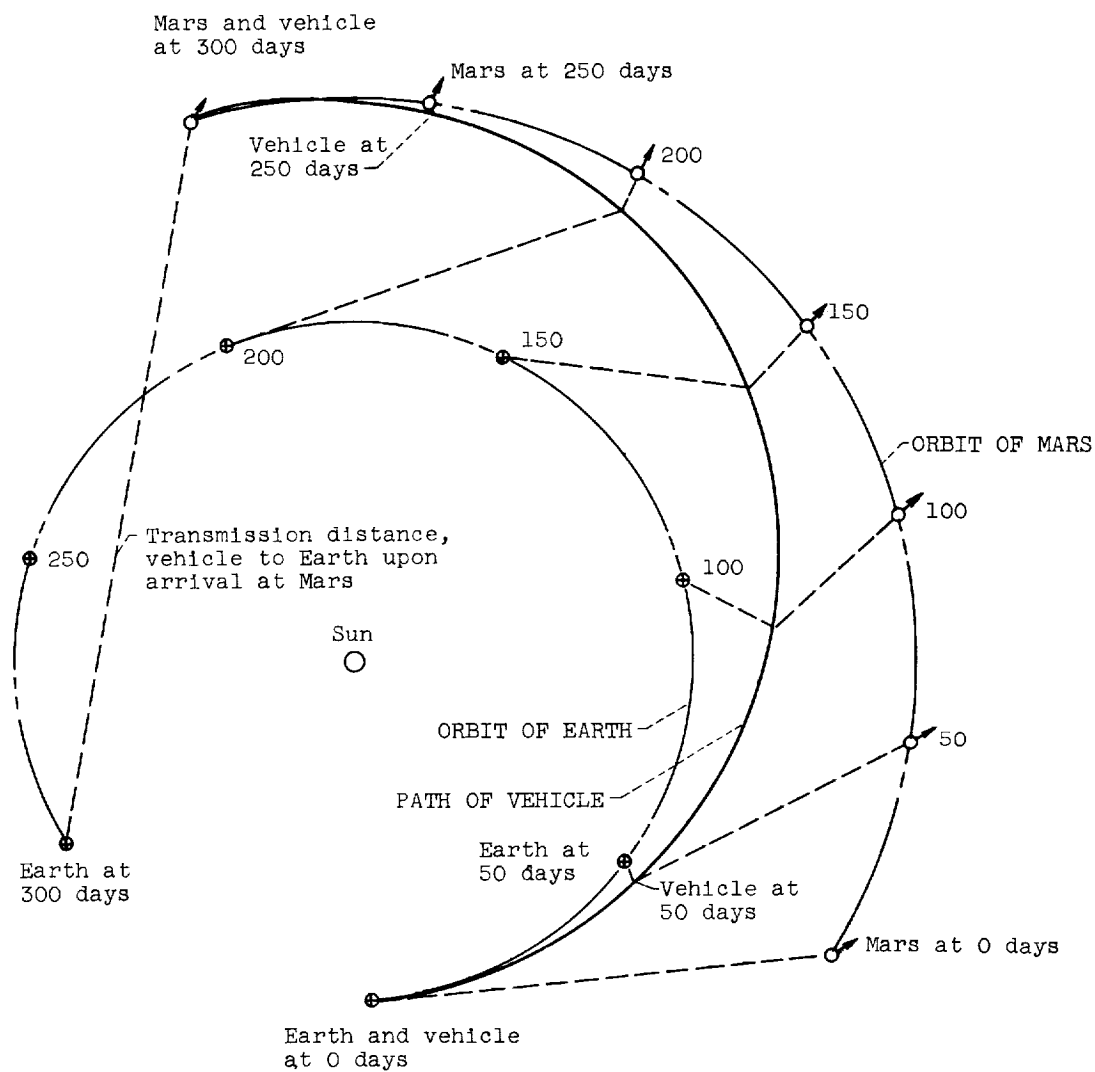
Items compared	Trip times investigated, days			
	150		300	
	n-Body value	Difference based on n-body, percent	n-Body value	Difference based on n-body, percent
Geocentric escape hyperbola				
Longitude of node, η_N	5.730°	Given	5.730°	Given
Orbital longitude of perigee, ω	19.959°	-0.976	-36.850°	-3.445
Semilatus rectum, p	13047.54 miles	-0.472	9531.933 miles	-0.747
Eccentricity, e	1.993	-0.786	1.186	-1.377
Inclination, i_e	38.827°	-0.085	11.232°	-2.636
Depart perigee velocity, V_p	8.089 miles/sec	-0.262	6.914 miles/sec	-0.374
Depart velocity increment, ΔV_p	3.413 miles/sec	-0.621	2.238 miles/sec	-1.157
Arrival perigee velocity, V_D	7.587 miles/sec	-0.028	3.416 miles/sec	-0.188
Arrival velocity increment, ΔV_D	5.482 miles/sec	-0.039	1.311 miles/sec	-0.491
Total velocity increment, ΔV_{tot}	8.895 miles/sec	-0.660	3.549 miles/sec	-1.647



(a) 150-Day trip.

Figure 1. - Position of vehicle with respect to Earth and Mars during typical 150- and 300-day trips to Mars.

E-1451



(b) 300-Day trip.

Figure 1. - Concluded. Position of vehicle with respect to Earth and Mars during typical 150- and 300-day trips to Mars.

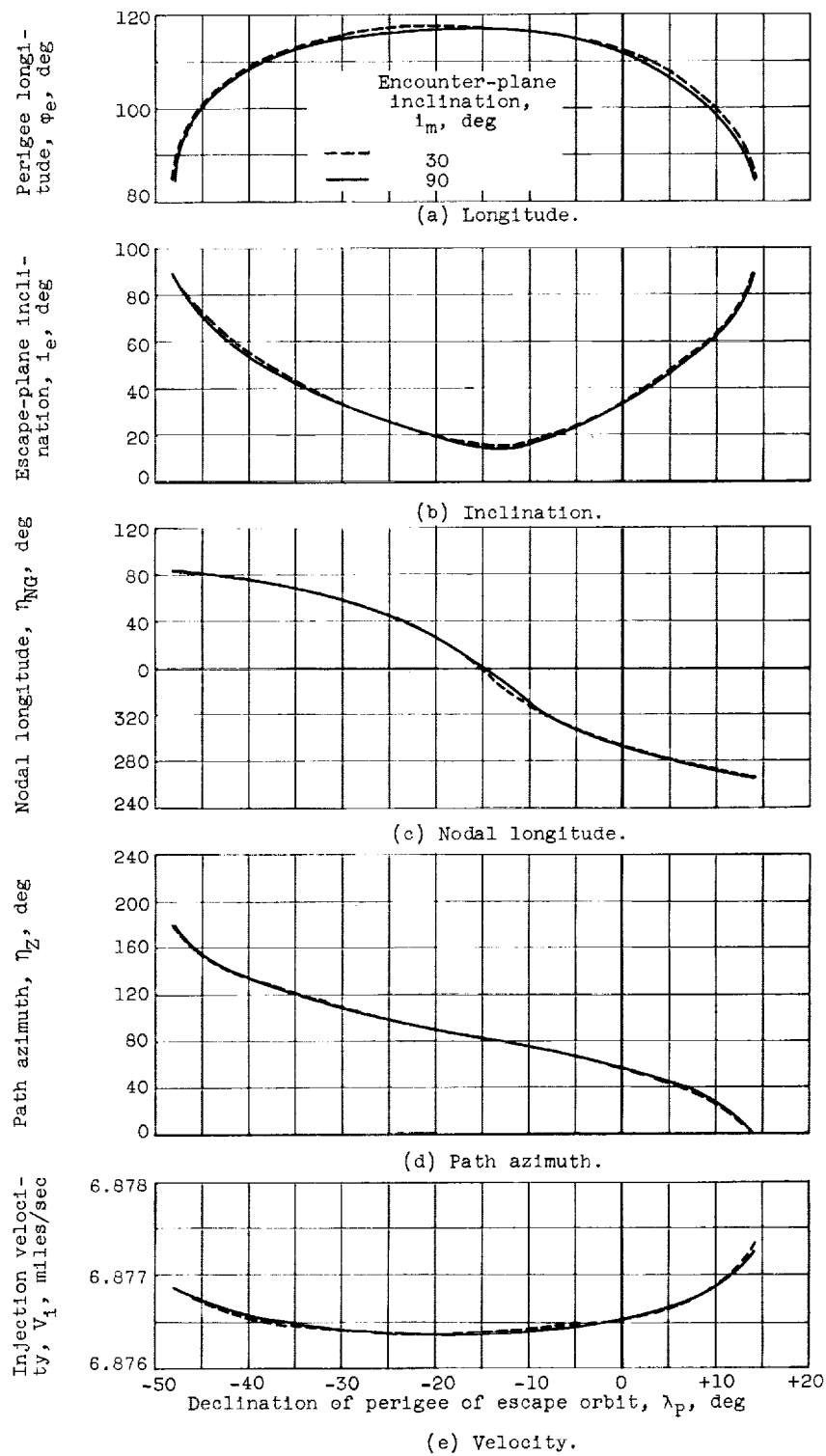


Figure 2. - Path parameters at perigee injection for Earth-Mars trip. Injection time, October 19, 1962 (Greenwich noon); trip time, T_{tot} , 300 days; encounter-plane inclination, 30° ; arrival trajectory angle, 0° .

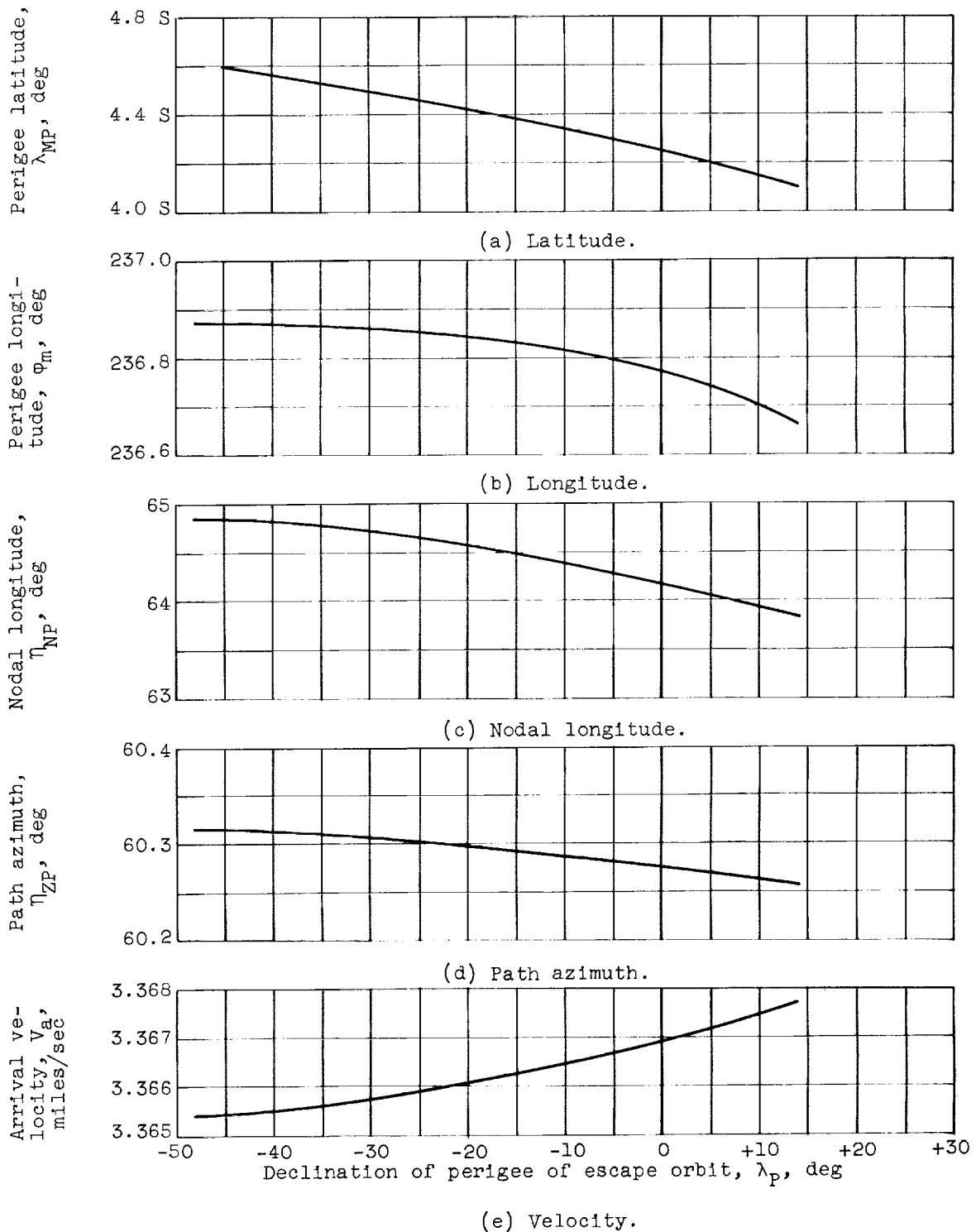


Figure 3. - Effect of geocentric escape plane inclination on path parameters at perigee of encounter hyperbola. Injection time, October 19, 1962 (Greenwich noon); trip time, T_{tot} , 300 days; encounter-plane inclination, 30° ; arrival trajectory angle, 0° .

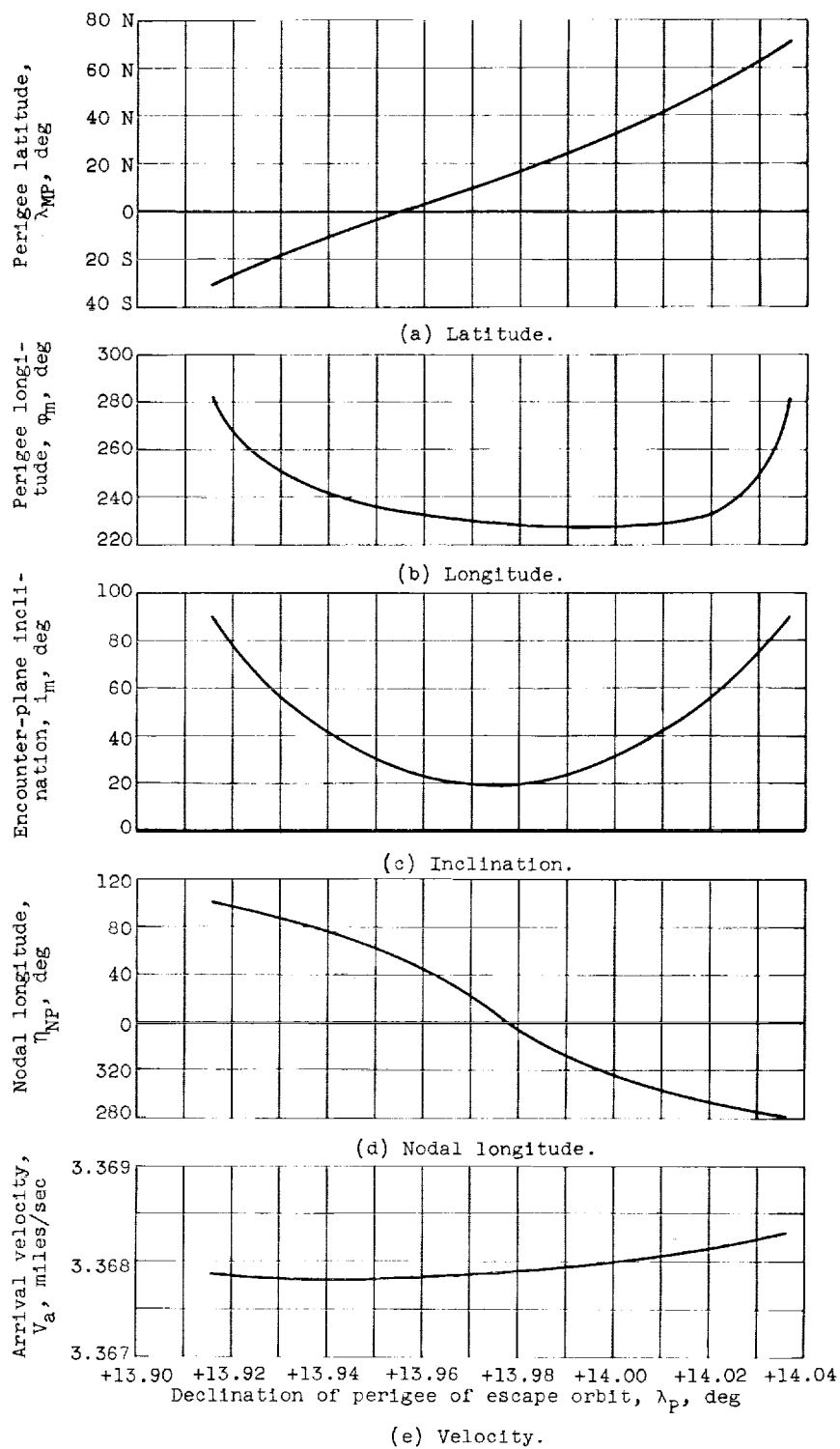


Figure 4. - Effect of encounter-plane inclination on path parameters at perigee of encounter hyperbola. Injection time, October 19, 1962 (Greenwich noon); trip time, T_{tot} , 300 days; escape-plane inclination, 90° ; injection trajectory angle, 0° .

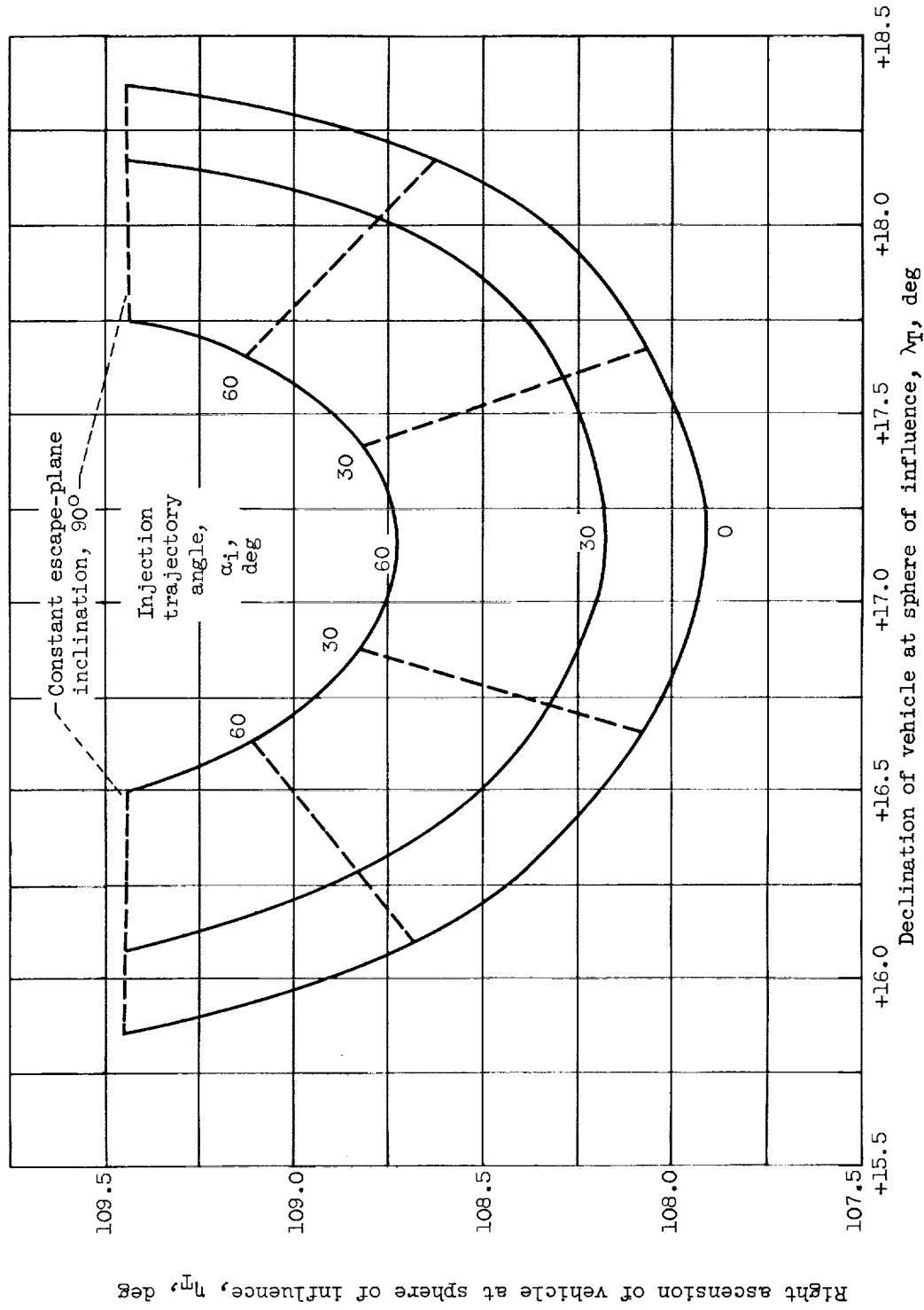


Figure 5. - Effect of injection trajectory angle at 1.1 Earth radii on coordinates of sphere-of-influence departure point. Injection time, October 19, 1962 (Greenwich noon); trip time, T_{tot} , 300 days; encounter-plane inclination, 90° ; arrival trajectory angle, 0° .

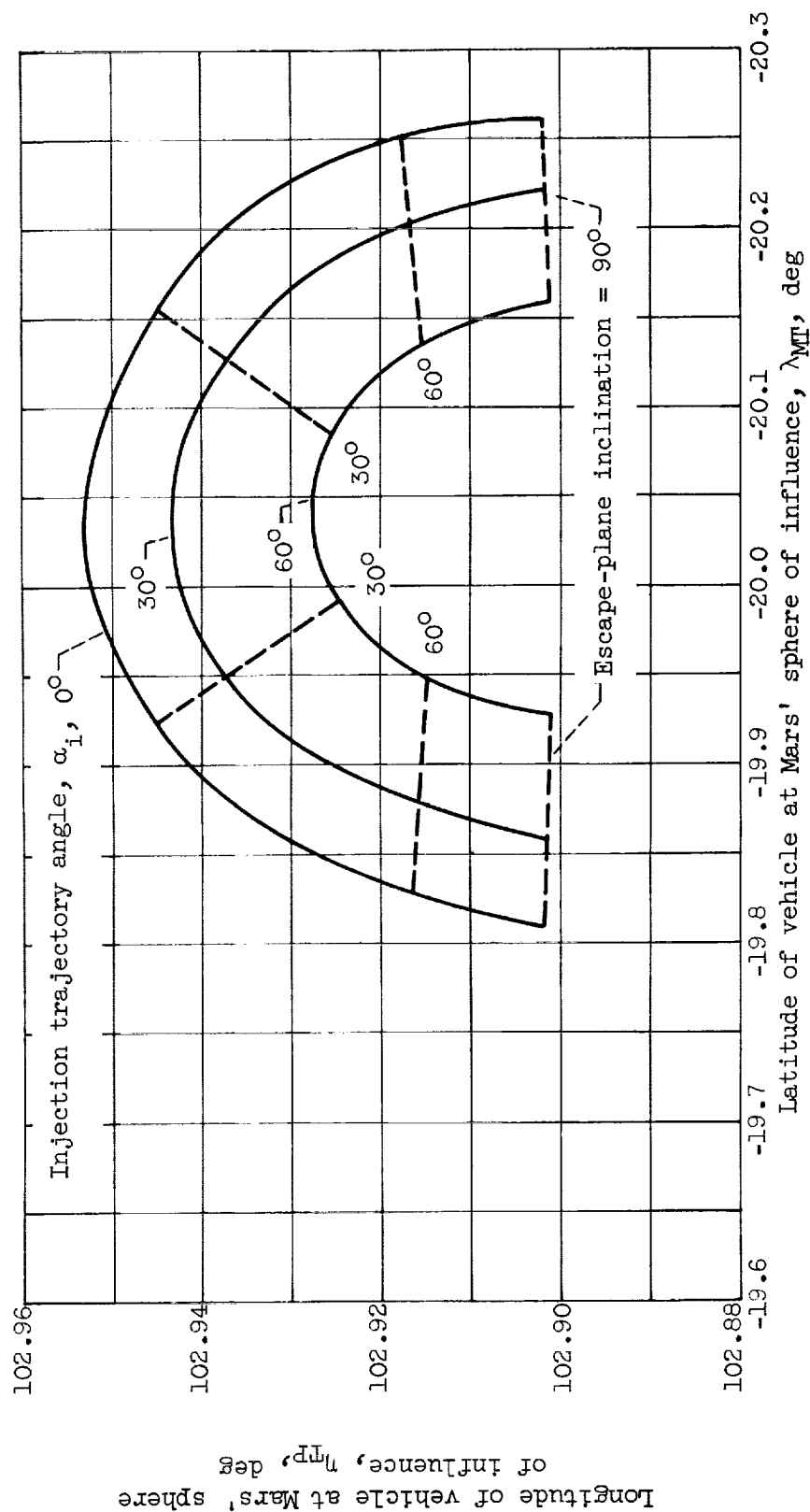


Figure 6. - Effect of injection trajectory angle at 1.1 Earth radii on coordinates of sphere-of-influence encounter point. Injection time, October 19, 1962 (Greenwich noon); trip time, T_{tot} , 300 days; encounter-plane inclination, 90°; arrival trajectory angle, 0°.

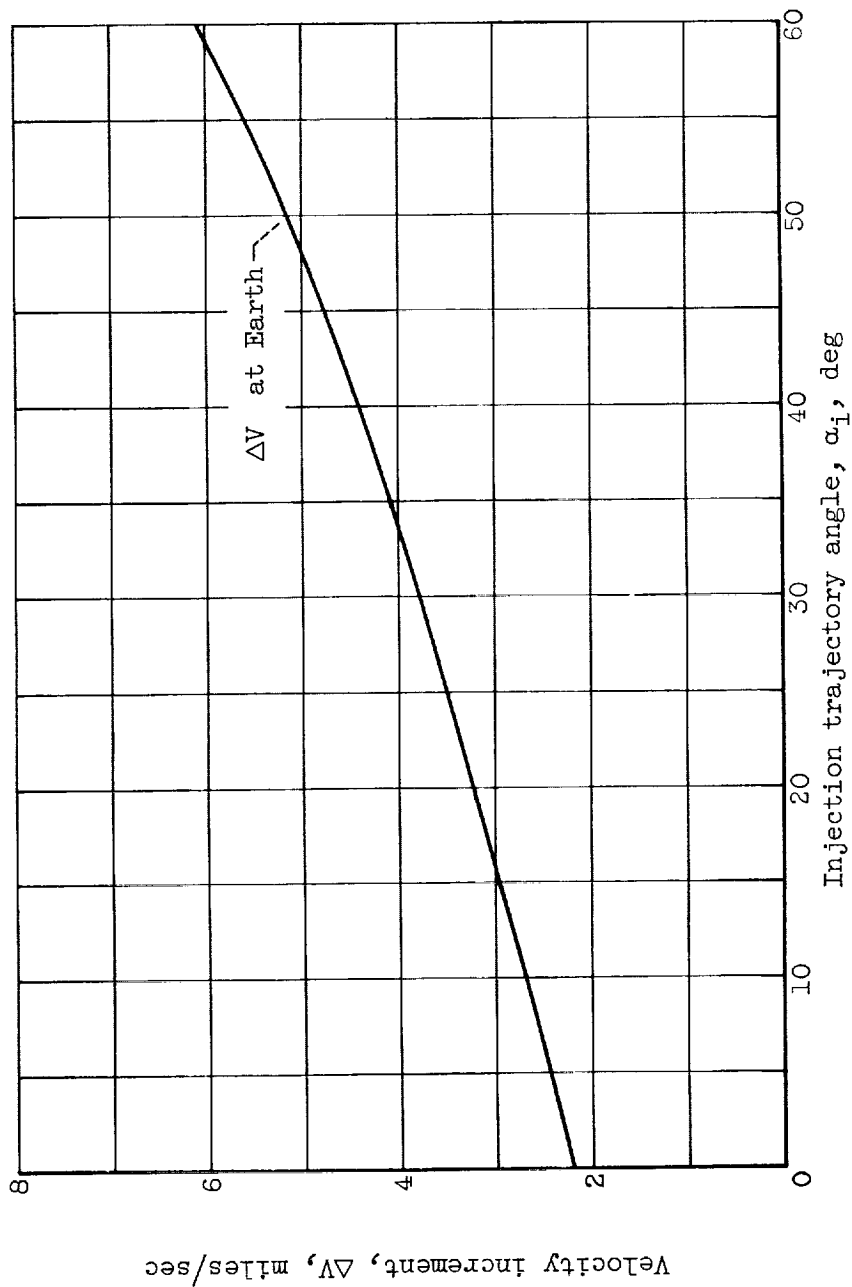


Figure 7. - Effect of injection trajectory angle at 1.1 Earth radii on injection velocity-increment requirements. Injection time, October 19, 1962 (Greenwich noon); trip time, T_{tot} , 300 days.

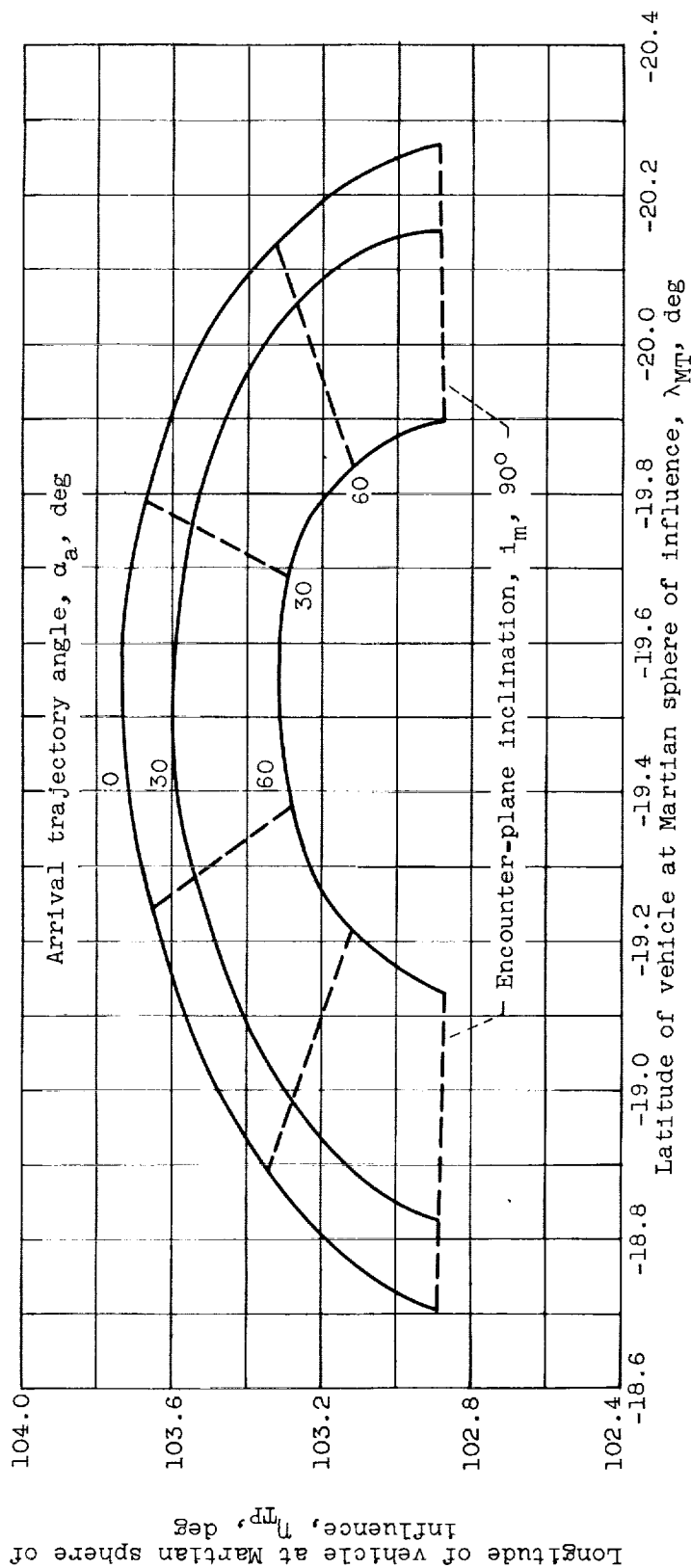


Figure 8. - Effect of arrival trajectory angle at 1.1 Mars radii on coordinates of sphere-of-influence encounter point. Injection time, October 19, 1962 (Greenwich noon); trip time, T_{tot} , 300 days; escape-plane inclination, 006; injection trajectory angle, 000.

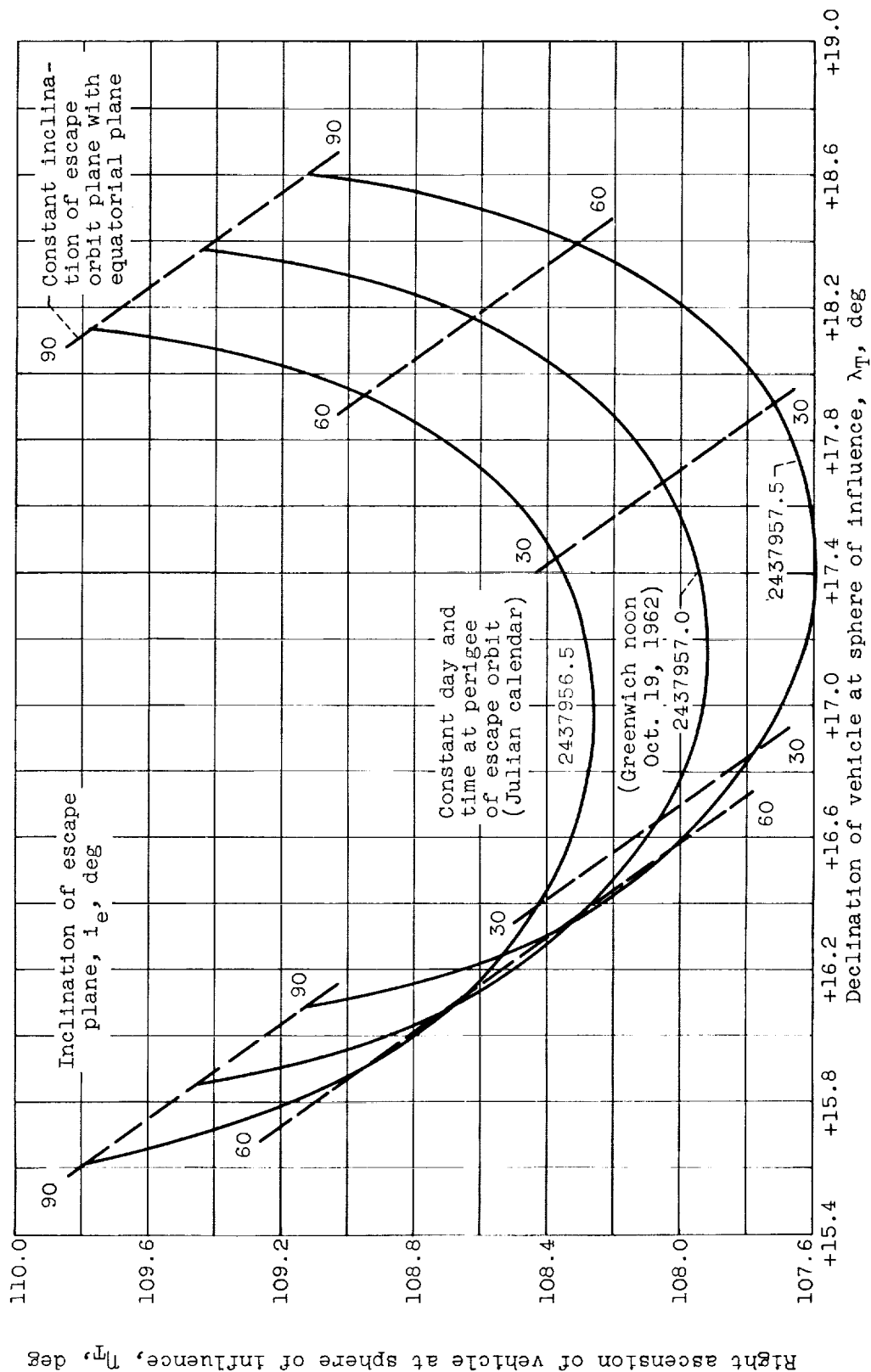
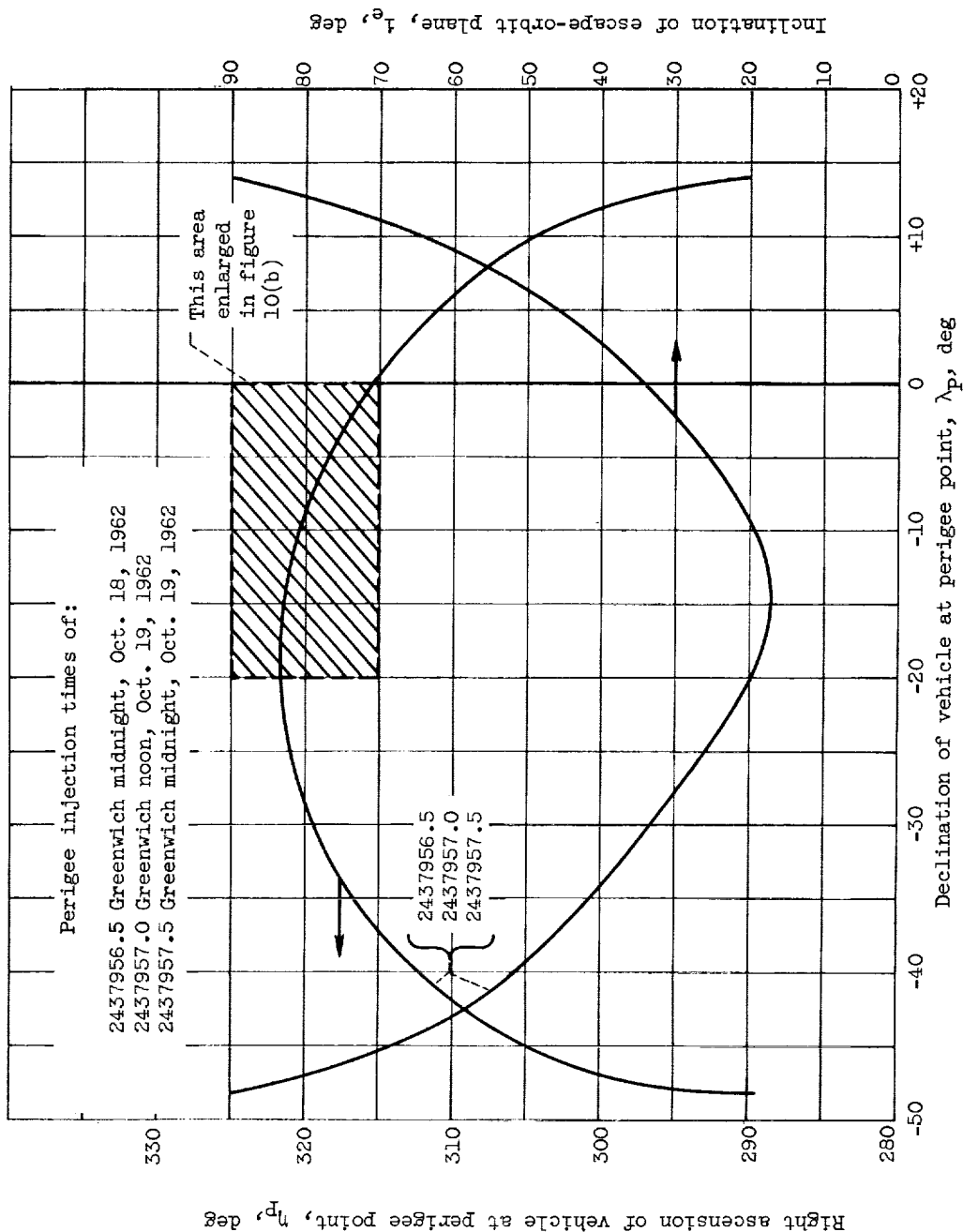
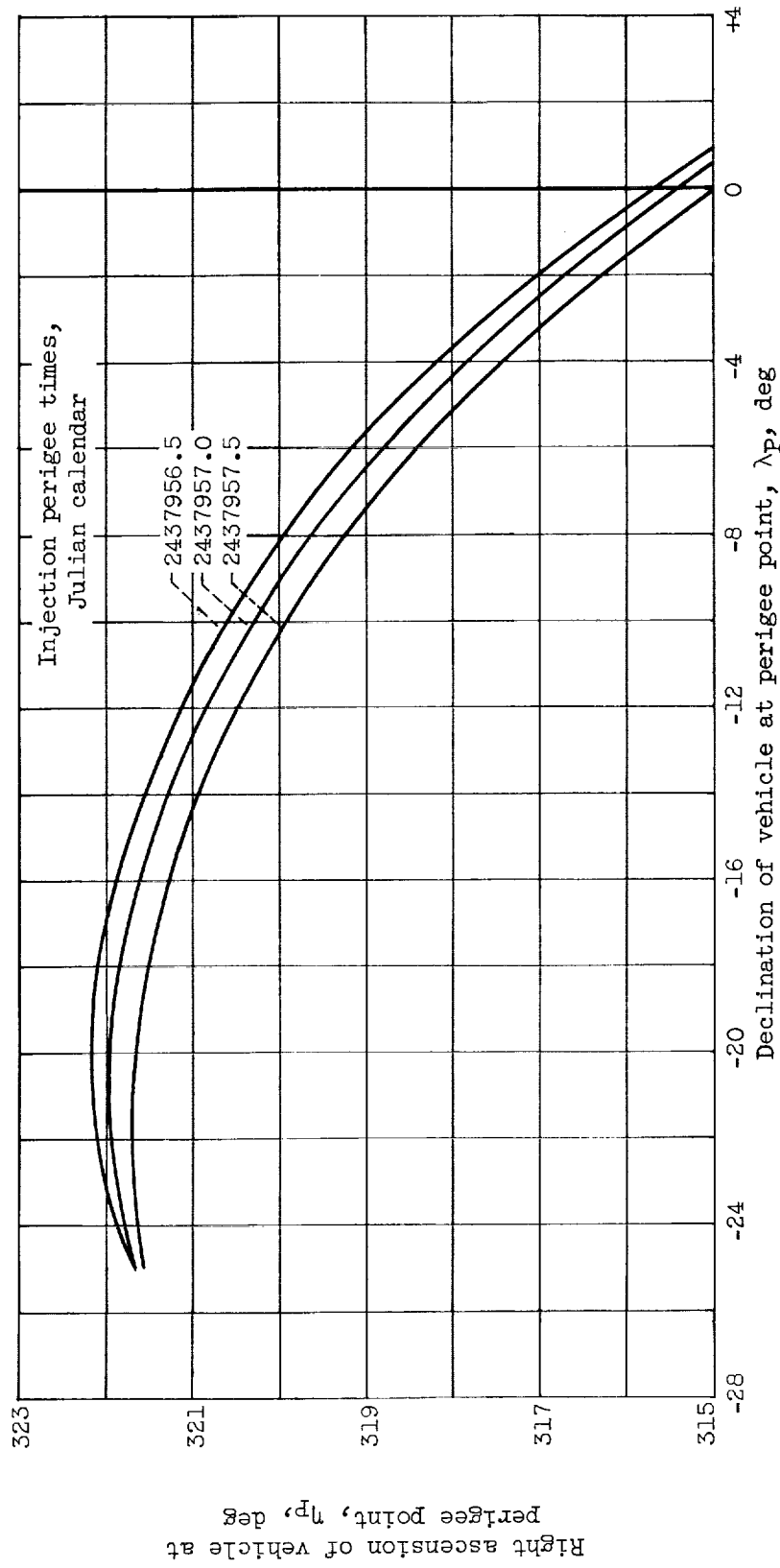


Figure 9. - Coordinates of sphere-of-influence departure point for 1-day span of perigee injection times. Trip time, T_{tot} , 300 days: encounter-plane inclination, 90°; arrival trajectory angle, 0°.



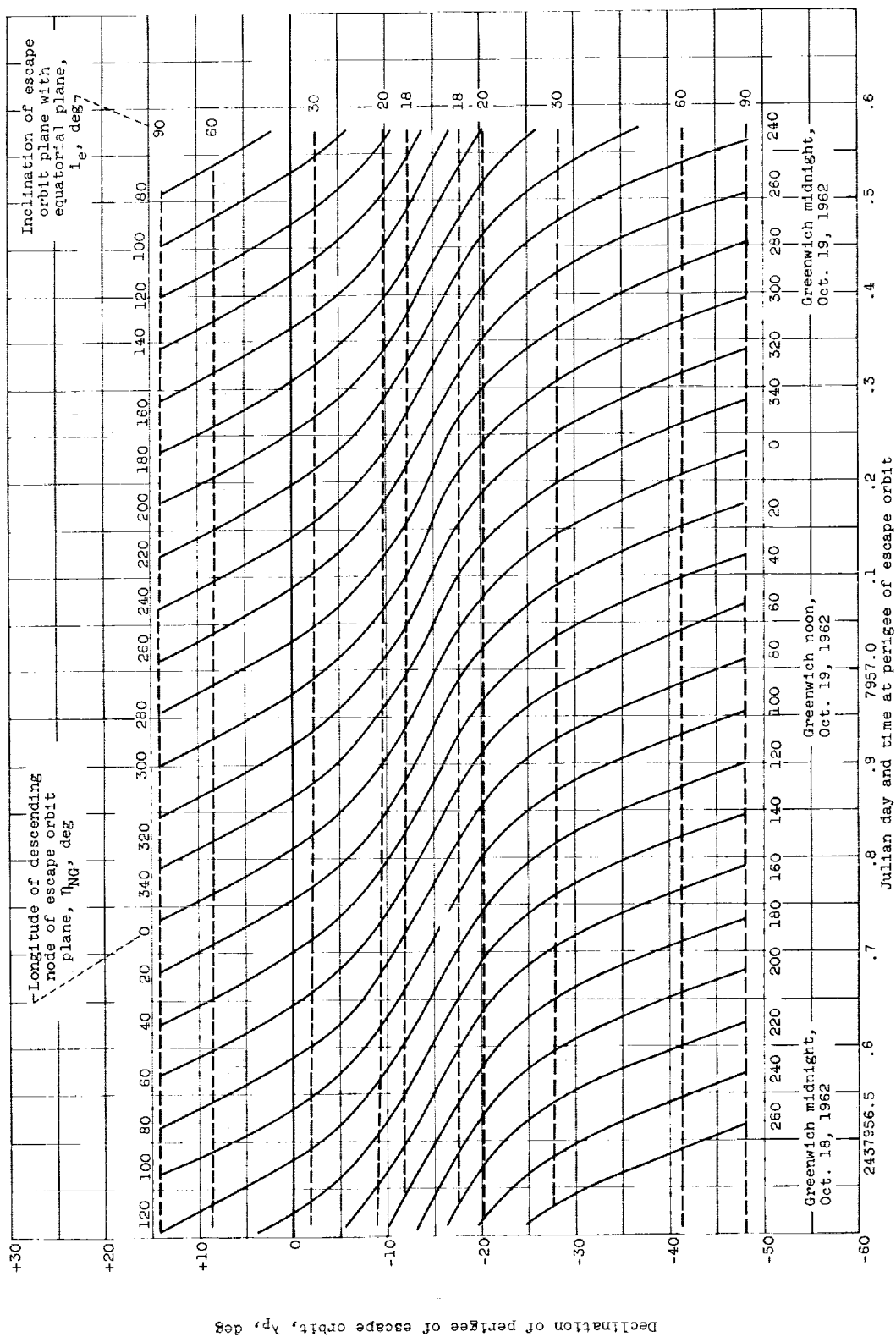
(a) Perigee right ascension and escape-plane inclination.

Figure 10. - Perigee injection parameters for Earth-Mars trip for 1-day span in injection time.



(b) Enlargement of portion of figure 10(a).

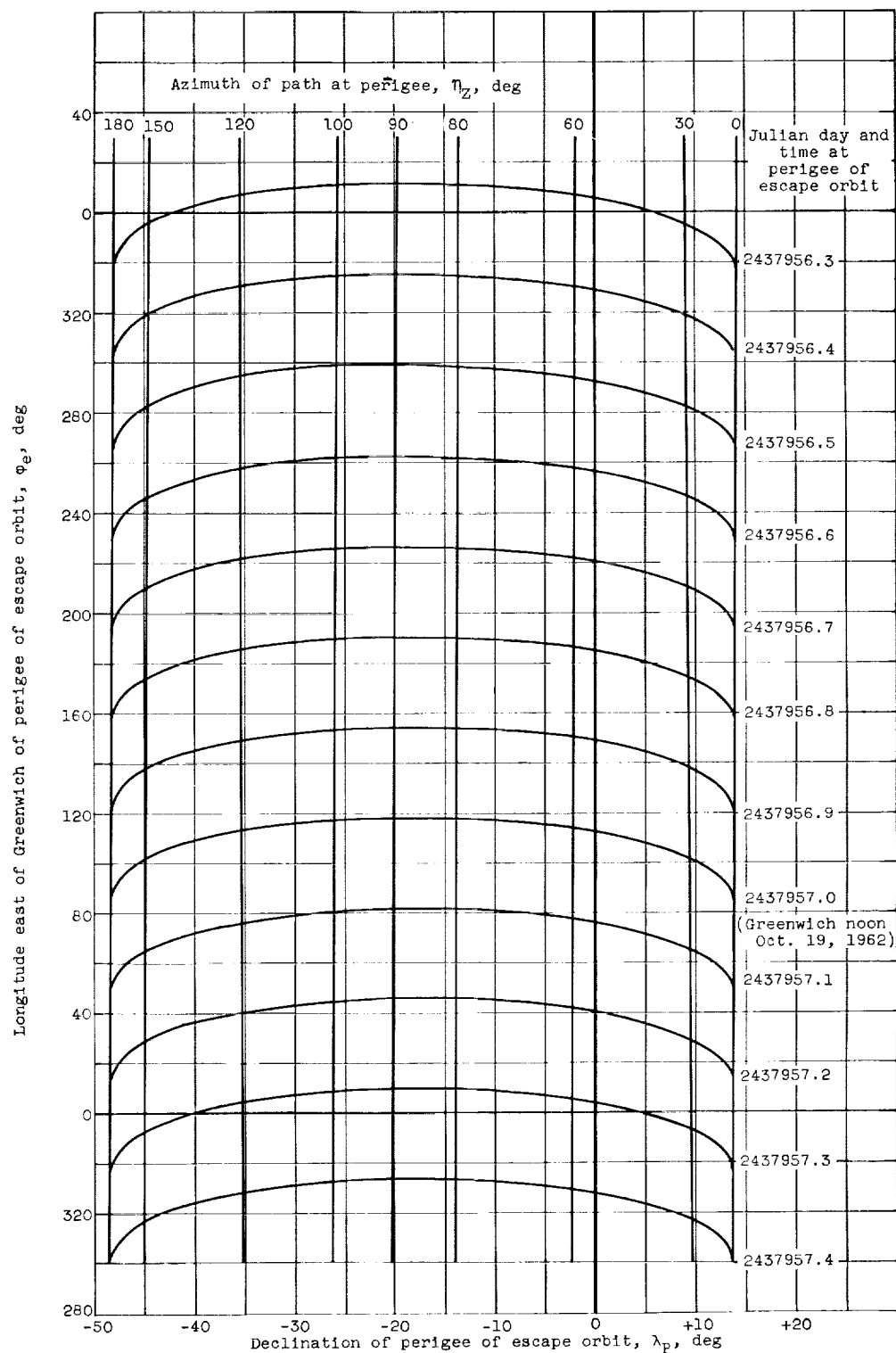
Figure 10. - Concluded. Perigee injection parameters for Earth-Mars trip for 1-day span in injection time.



(a) Escape-plane orientation and perigee injection-point declination.

Figure 11. - Geocentric escape-plane orientation and perigee injection requirements for a trip to Mars. Injection times over span of 1 day; trip time, T_{tot} , 300 days; encounter-plane inclination, 90°; arrival trajectory angle, 0°.

E-1451



(b) Longitude, azimuth, and time.

Figure 11. - Concluded. Geocentric escape-plane orientation and perigee injection requirements for a trip to Mars. Injection times over span of 1 day; trip time, T_{tot} , 300 days; encounter-plane inclination, 90° ; arrival trajectory angle, 0° .

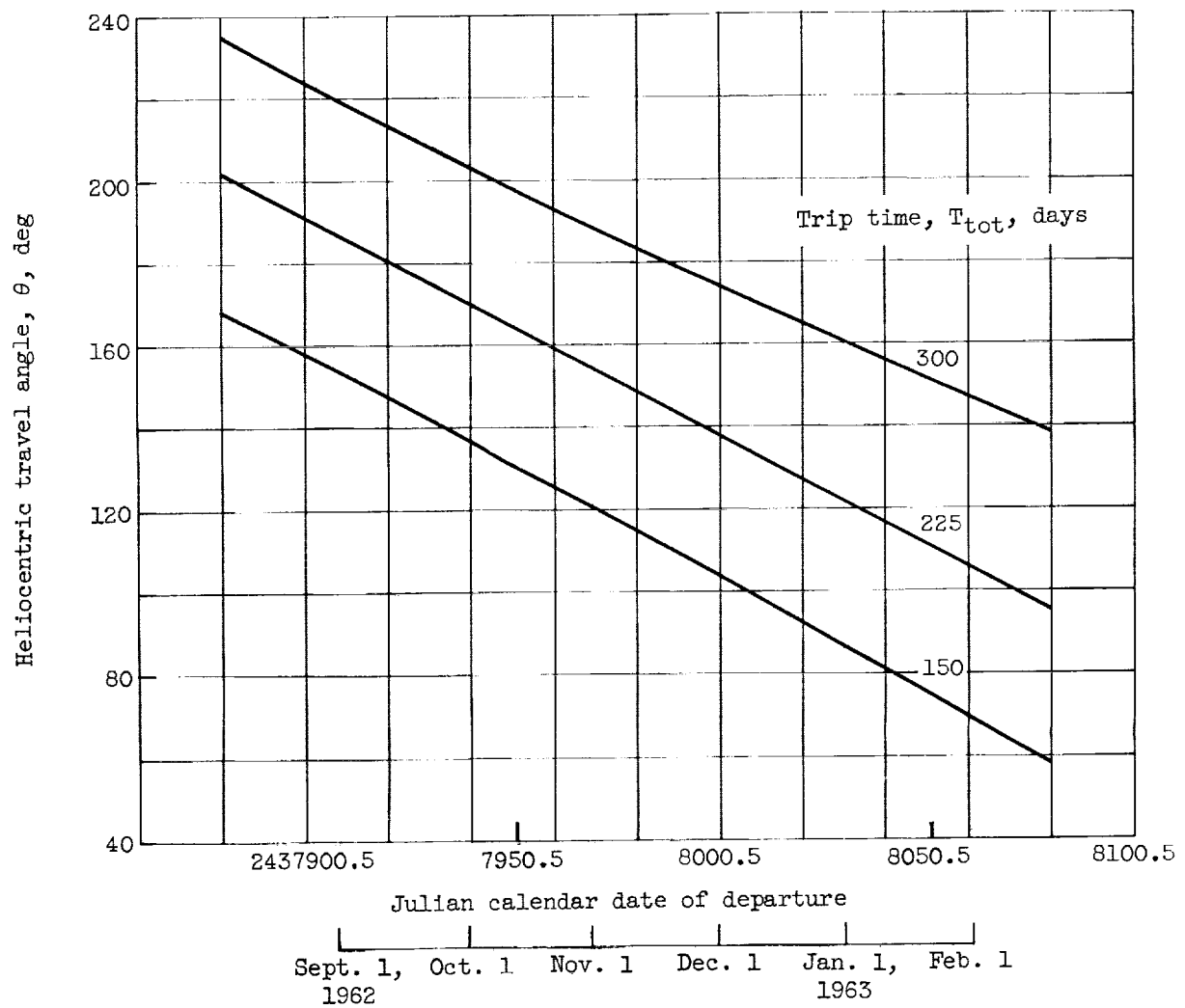


Figure 12. - Heliocentric travel angle for several trips to Mars with departures from Earth.

E-1451

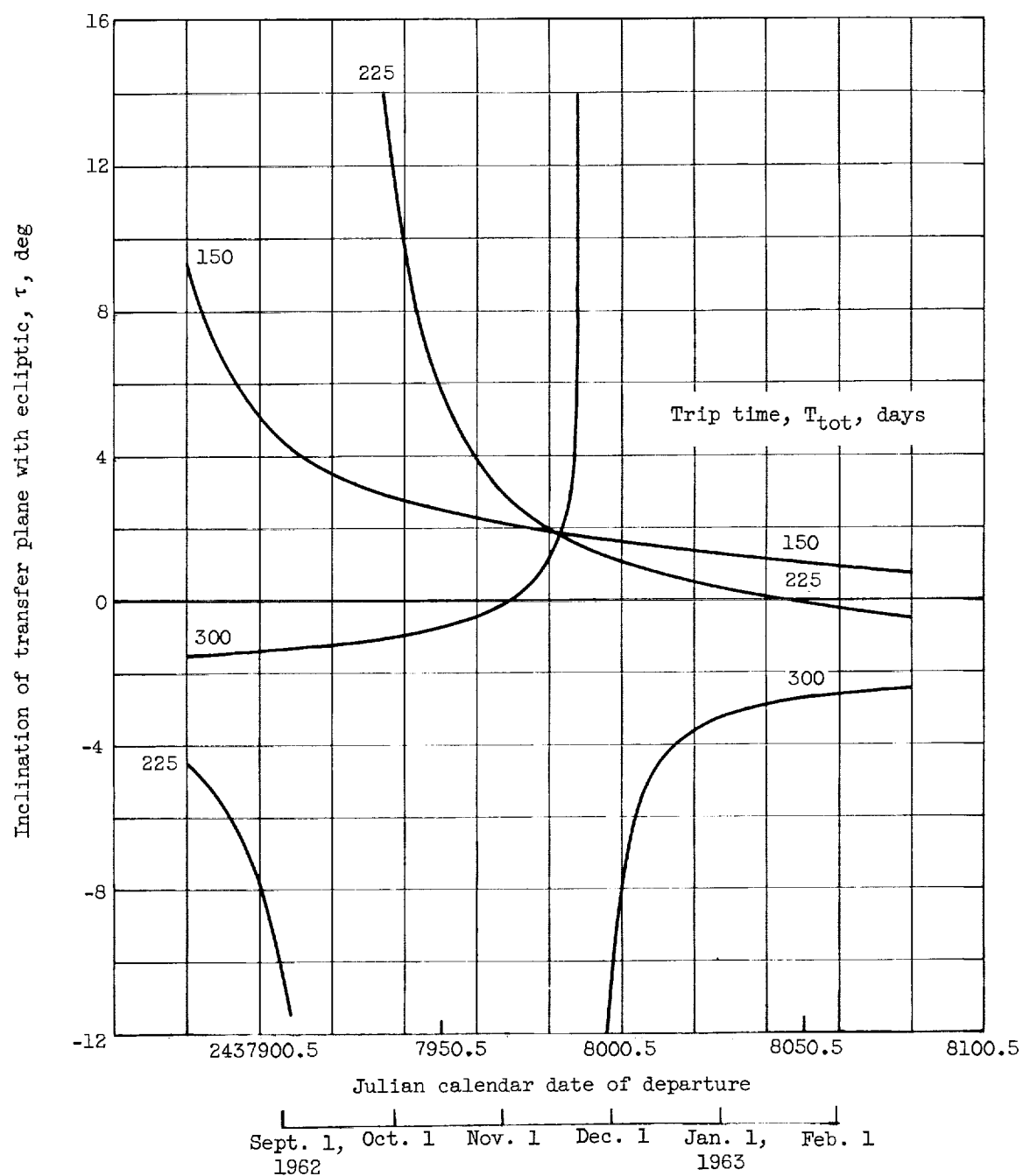


Figure 13. - Inclination of heliocentric transfer plane with respect to ecliptic plane for several trips to Mars with departures from Earth in 1962-63.

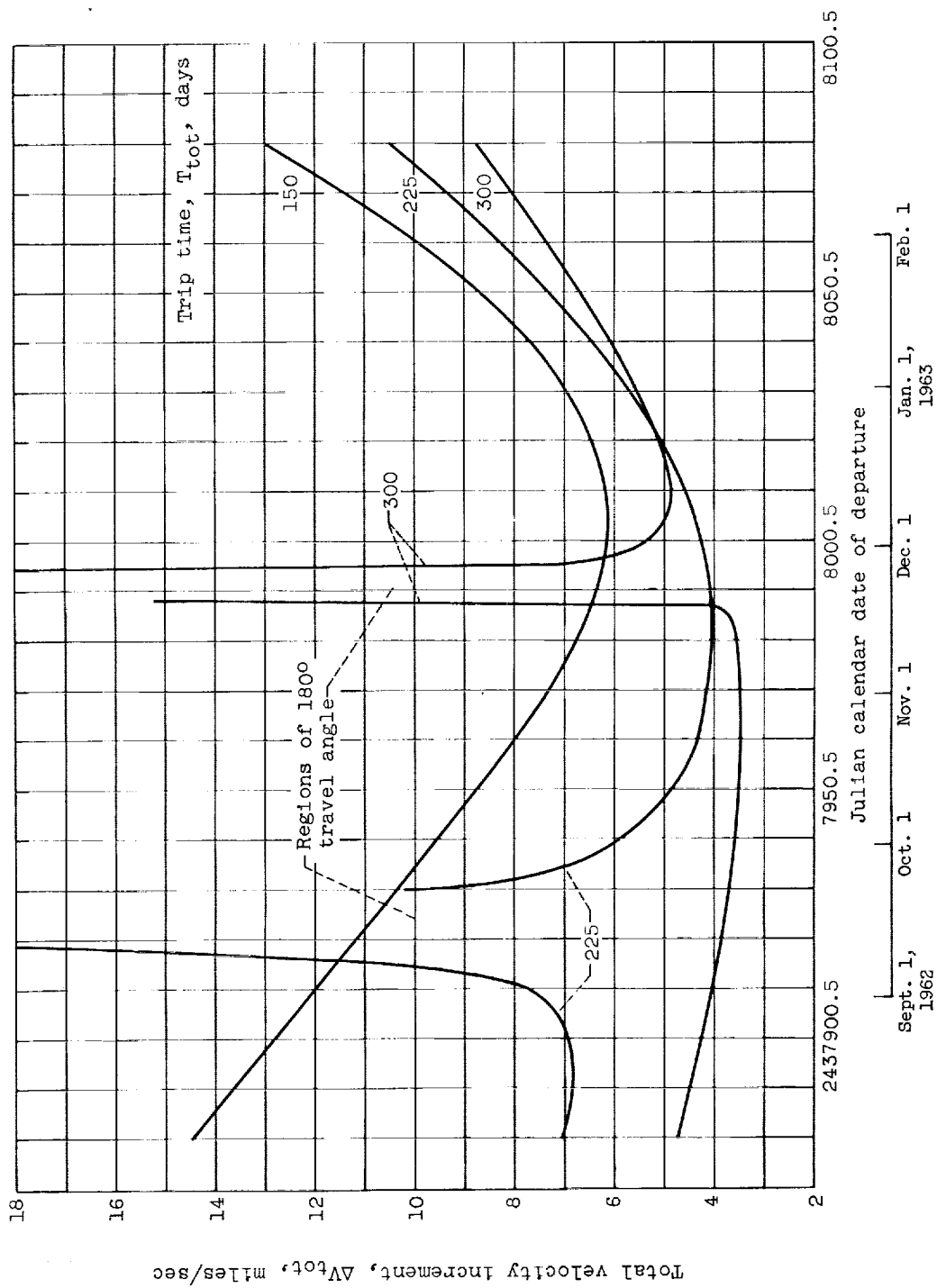


Figure 14. - Total velocity-increment requirements for several trips to Mars in 1962-63 starting and ending in circular orbits at 1.1 planet radii.

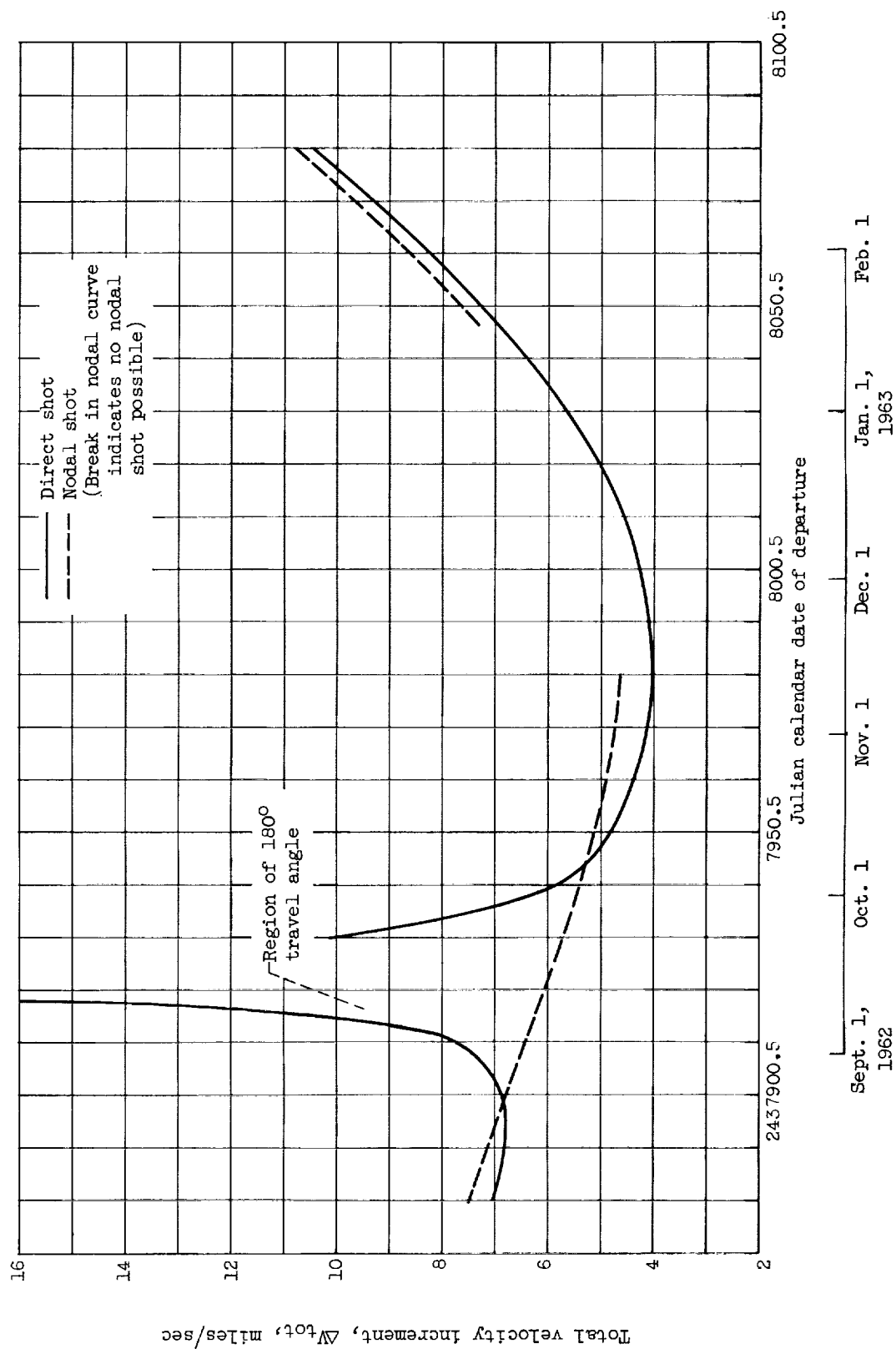


Figure 15. - Comparison of total velocity increments for nodal- and direct-type 225-day trips to Mars starting and ending in circular orbits at 1.1 planet radii.

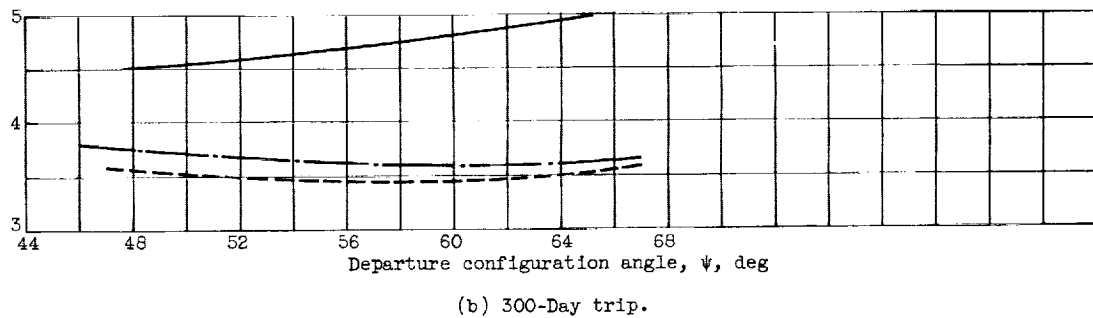
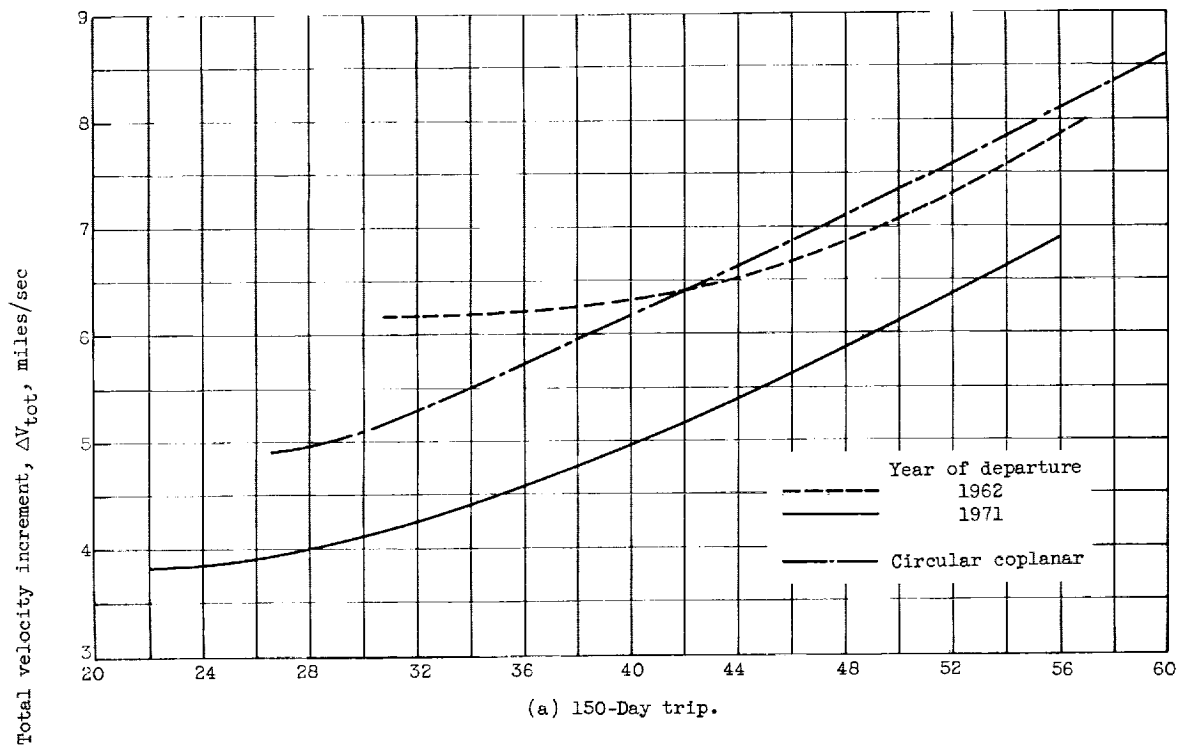
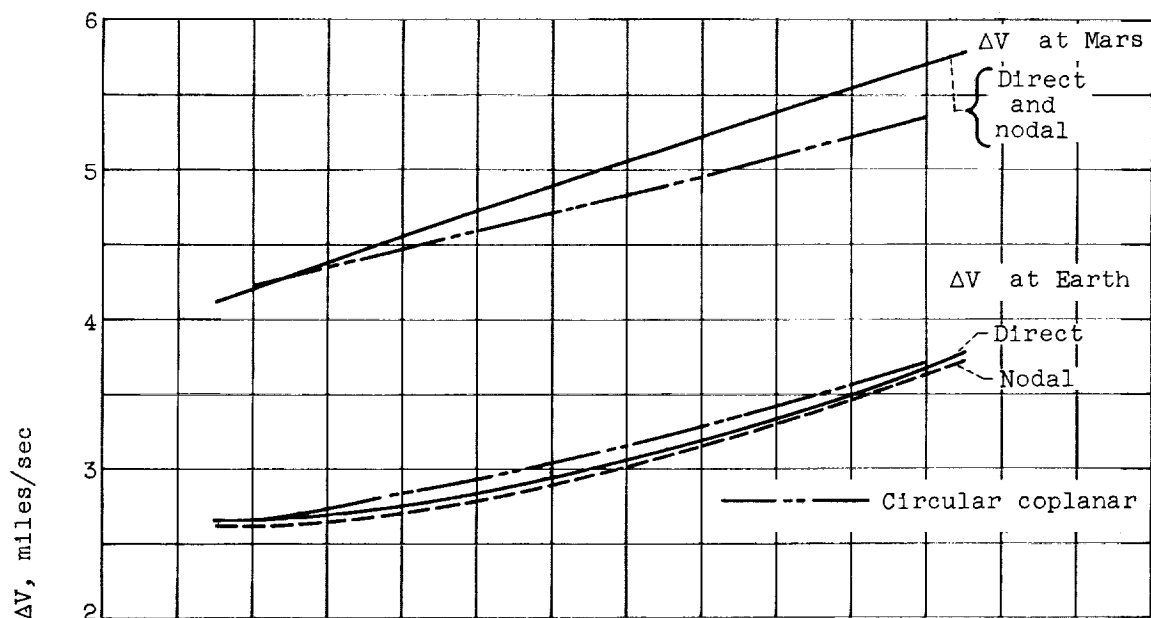
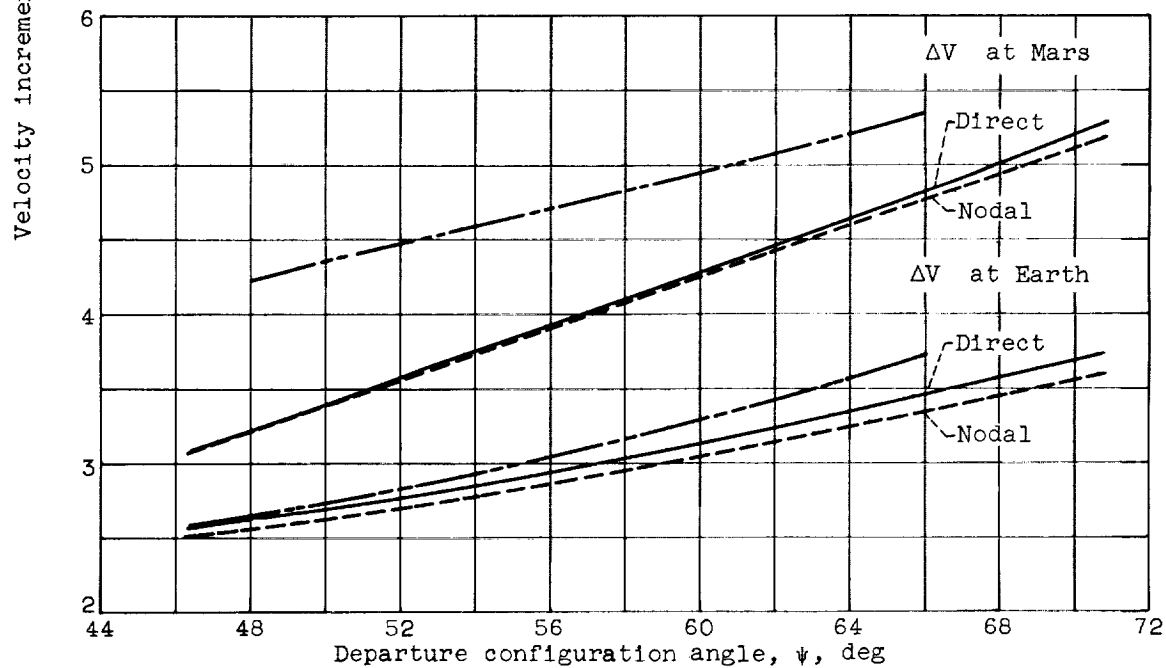


Figure 16. - Comparison of total velocity increments for trips to Mars in 1962 and 1971, starting and ending in circular orbits at 1.1 planet radii.

E-1451

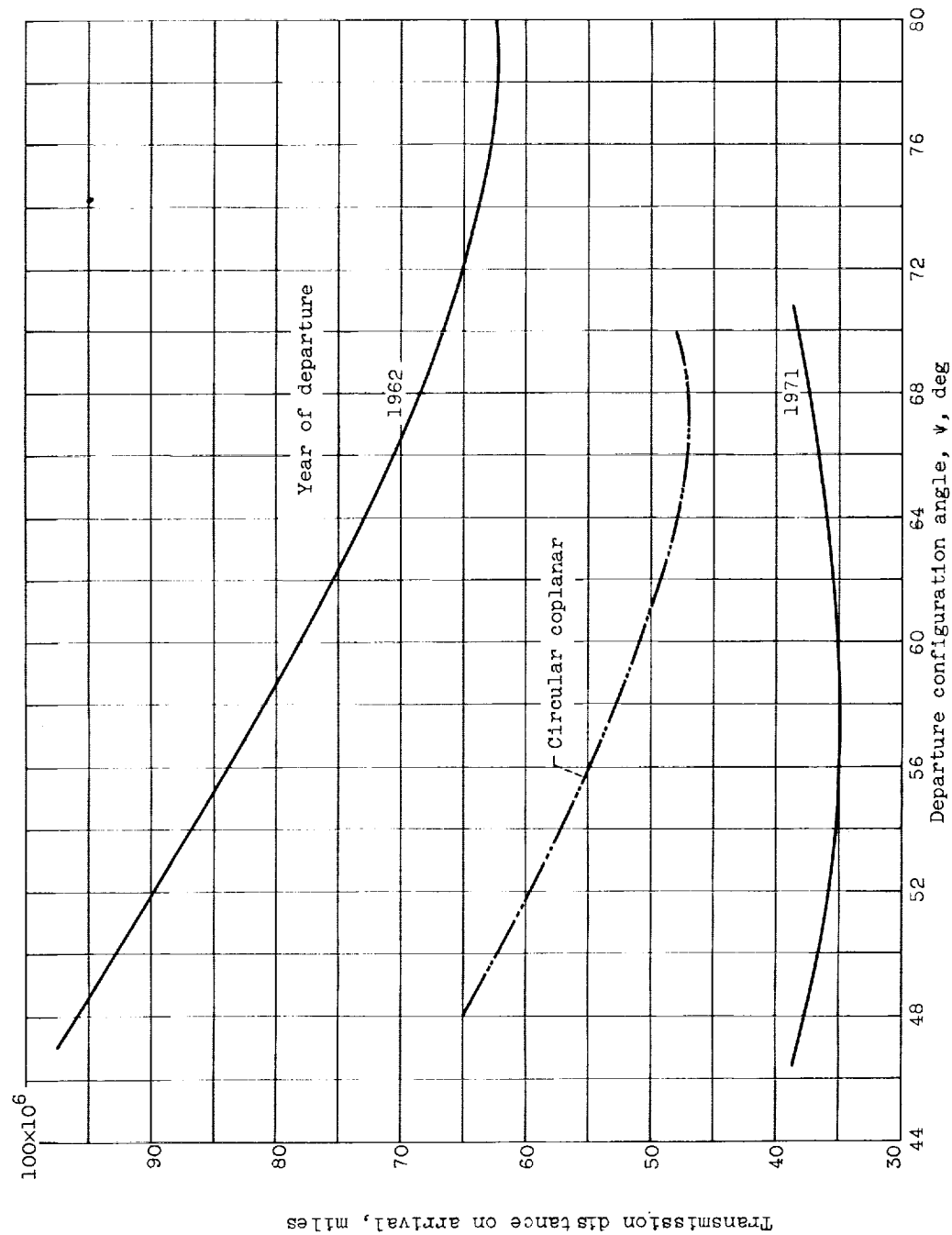


(a) Departure in 1962.



(b) Departure in 1971.

Figure 17. - Comparison of velocity increments required at Earth and Mars, starting and ending in circular orbits at 1.1 planet radii for a 150-day nodal- and direct-type trip.



(a) 150-Day trip.

Figure 18. - Comparison of circular-coplanar and three-dimensional arrival transmission distance for trips to Mars in 1962 and 1971.

E-1451

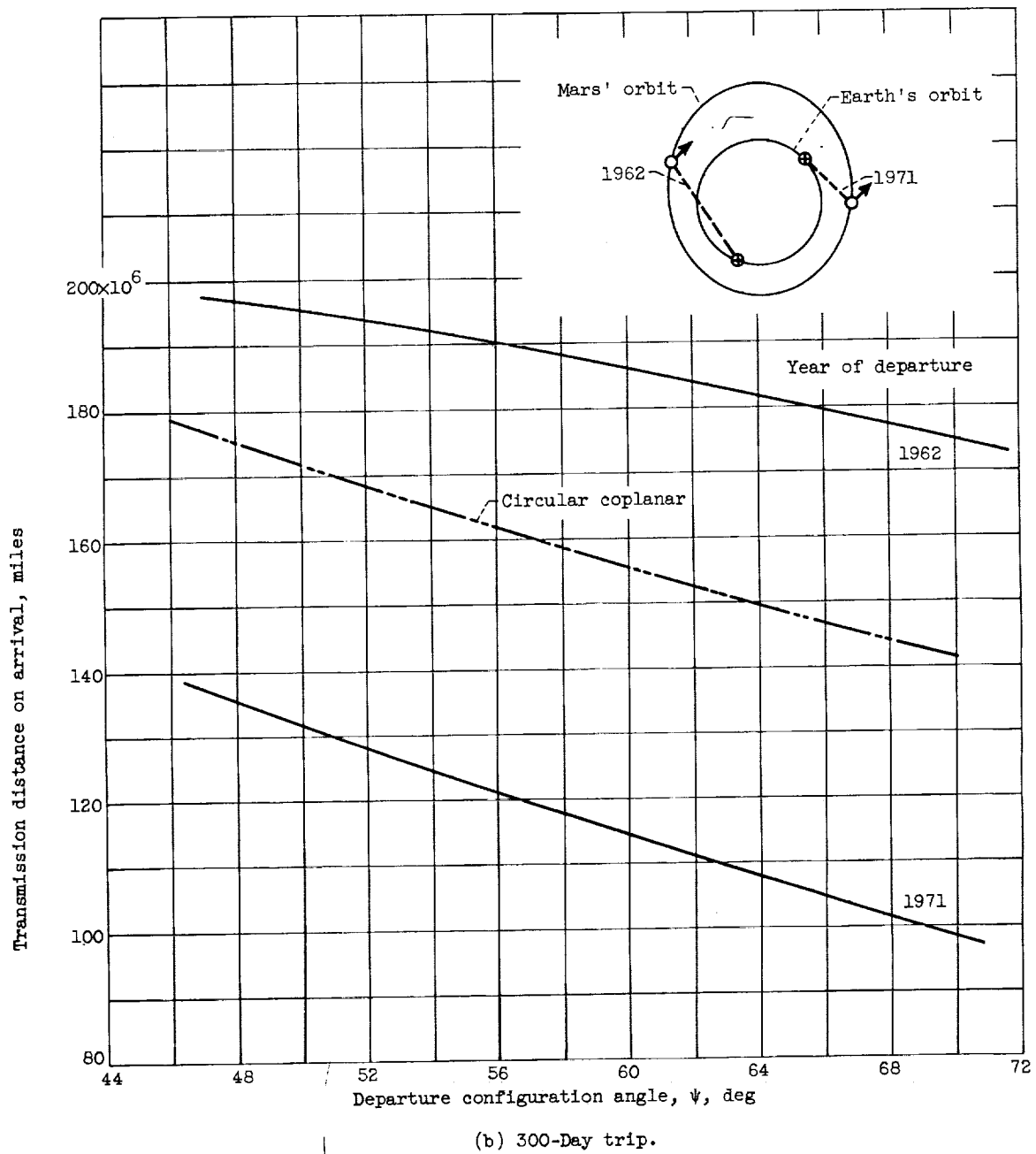


Figure 18. - Concluded. Comparison of circular-coplanar and three-dimensional arrival transmission distance for trips to Mars in 1962 and 1971.

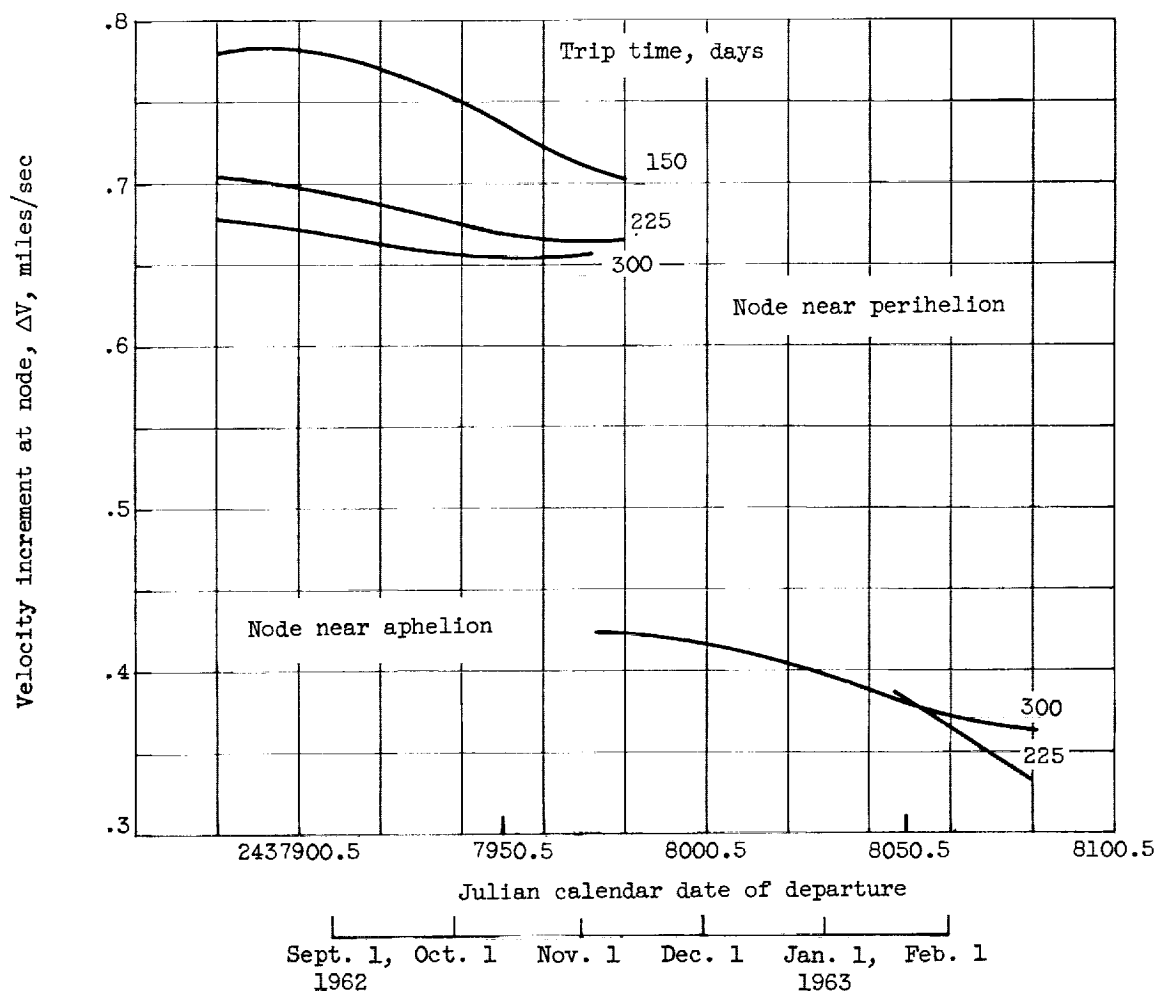


Figure 19. - Velocity increment required at node of Martian orbital plane and ecliptic plane to effect plane change on nodal-type shot from Earth to Mars. Note: Nodal shot not possible for span of departure dates for 150- and 225-day trips.

<p>NASA TN D-1199 National Aeronautics and Space Administration. THREE-DIMENSIONAL SPHERE-OF-INFLUENCE ANALYSIS OF INTERPLANETARY TRAJECTORIES TO MARS. Gerald Knip, Jr., and Charles L. Zola. May 1962. 68p. OTS price, \$1.75. (NASA TECHNICAL NOTE D-1199)</p> <p>The method of analysis, for which equations are presented, employs arbitrary spheres to differentiate planetocentric and heliocentric motion. For a trip of fixed duration, planetocentric parameters such as escape- and encounter-plane inclination, injection and arrival trajectory angles, and injection time were varied to determine their effects on injection-point coordinates and mission velocity-increment requirements. Trips of 150-, 225-, and 300-day duration were used to investigate the relations among velocity-increment requirements, departure date, trip time, communication distance, heliocentric transfer-plane inclination, and synodic period of departure. These data are compared with circular-coplanar results.</p>	<p>I. Knip, Gerald, Jr. II. Zola, Charles L. III. NASA TN D-1199</p> <p>(Initial NASA distribution: 2, Aerodynamics, missiles and space vehicles; 23, Launching facilities and operations; 24, Launching dynamics; 28, Missiles and satellite carriers; 46, Space mechanics.)</p> <p>NASA</p>	<p>NASA TN D-1199 National Aeronautics and Space Administration. THREE-DIMENSIONAL SPHERE-OF-INFLUENCE ANALYSIS OF INTERPLANETARY TRAJECTORIES TO MARS. Gerald Knip, Jr., and Charles L. Zola. May 1962. 68p. OTS price, \$1.75. (NASA TECHNICAL NOTE D-1199)</p> <p>The method of analysis, for which equations are presented, employs arbitrary spheres to differentiate planetocentric and heliocentric motion. For a trip of fixed duration, planetocentric parameters such as escape- and encounter-plane inclination, injection and arrival trajectory angles, and injection time were varied to determine their effects on injection-point coordinates and mission velocity-increment requirements. Trips of 150-, 225-, and 300-day duration were used to investigate the relations among velocity-increment requirements, departure date, trip time, communication distance, heliocentric transfer-plane inclination, and synodic period of departure. These data are compared with circular-coplanar results.</p>	<p>I. Knip, Gerald, Jr. II. Zola, Charles L. III. NASA TN D-1199</p> <p>(Initial NASA distribution: 2, Aerodynamics, missiles and space vehicles; 23, Launching facilities and operations; 24, Launching dynamics; 28, Missiles and satellite carriers; 46, Space mechanics.)</p> <p>NASA</p>
<p>NASA TN D-1199 National Aeronautics and Space Administration. THREE-DIMENSIONAL SPHERE-OF-INFLUENCE ANALYSIS OF INTERPLANETARY TRAJECTORIES TO MARS. Gerald Knip, Jr., and Charles L. Zola. May 1962. 68p. OTS price, \$1.75. (NASA TECHNICAL NOTE D-1199)</p> <p>The method of analysis, for which equations are presented, employs arbitrary spheres to differentiate planetocentric and heliocentric motion. For a trip of fixed duration, planetocentric parameters such as escape- and encounter-plane inclination, injection and arrival trajectory angles, and injection time were varied to determine their effects on injection-point coordinates and mission velocity-increment requirements. Trips of 150-, 225-, and 300-day duration were used to investigate the relations among velocity-increment requirements, departure date, trip time, communication distance, heliocentric transfer-plane inclination, and synodic period of departure. These data are compared with circular-coplanar results.</p>	<p>I. Knip, Gerald, Jr. II. Zola, Charles L. III. NASA TN D-1199</p> <p>(Initial NASA distribution: 2, Aerodynamics, missiles and space vehicles; 23, Launching facilities and operations; 24, Launching dynamics; 28, Missiles and satellite carriers; 46, Space mechanics.)</p> <p>NASA</p>	<p>NASA TN D-1199 National Aeronautics and Space Administration. THREE-DIMENSIONAL SPHERE-OF-INFLUENCE ANALYSIS OF INTERPLANETARY TRAJECTORIES TO MARS. Gerald Knip, Jr., and Charles L. Zola. May 1962. 68p. OTS price, \$1.75. (NASA TECHNICAL NOTE D-1199)</p> <p>The method of analysis, for which equations are presented, employs arbitrary spheres to differentiate planetocentric and heliocentric motion. For a trip of fixed duration, planetocentric parameters such as escape- and encounter-plane inclination, injection and arrival trajectory angles, and injection time were varied to determine their effects on injection-point coordinates and mission velocity-increment requirements. Trips of 150-, 225-, and 300-day duration were used to investigate the relations among velocity-increment requirements, departure date, trip time, communication distance, heliocentric transfer-plane inclination, and synodic period of departure. These data are compared with circular-coplanar results.</p>	<p>I. Knip, Gerald, Jr. II. Zola, Charles L. III. NASA TN D-1199</p> <p>(Initial NASA distribution: 2, Aerodynamics, missiles and space vehicles; 23, Launching facilities and operations; 24, Launching dynamics; 28, Missiles and satellite carriers; 46, Space mechanics.)</p> <p>NASA</p>

<p>NASA TN D-1199 National Aeronautics and Space Administration. THREE-DIMENSIONAL SPHERE-OF-INFLUENCE ANALYSIS OF INTERPLANETARY TRAJECTORIES TO MARS. Gerald Knip, Jr., and Charles L. Zola. May 1962. 68p. OTS price, \$1.75. (NASA TECHNICAL NOTE D-1199)</p> <p>The method of analysis, for which equations are presented, employs arbitrary spheres to differentiate planetocentric and heliocentric motion. For a trip of fixed duration, planetocentric parameters such as escape- and encounter-plane inclination, injection and arrival trajectory angles, and injection time were varied to determine their effects on injection-point coordinates and mission velocity-increment requirements. Trips of 150-, 225-, and 300-day duration were used to investigate the relations among velocity-increment requirements, departure date, trip time, communication distance, heliocentric transfer-plane inclination, and synodic period of departure. These data are compared with circular-coplanar results.</p>	<p>I. Knip, Gerald, Jr. II. Zola, Charles L. III. NASA TN D-1199</p> <p>(Initial NASA distribution: 2, Aerodynamics, missiles and space vehicles; 23, Launching facilities and operations; 24, Launching dynamics; 28, Missiles and satellite carriers; 46, Space mechanics.)</p>	NASA
<p>NASA TN D-1199 National Aeronautics and Space Administration. THREE-DIMENSIONAL SPHERE-OF-INFLUENCE ANALYSIS OF INTERPLANETARY TRAJECTORIES TO MARS. Gerald Knip, Jr., and Charles L. Zola. May 1962. 68p. OTS price, \$1.75. (NASA TECHNICAL NOTE D-1199)</p> <p>The method of analysis, for which equations are presented, employs arbitrary spheres to differentiate planetocentric and heliocentric motion. For a trip of fixed duration, planetocentric parameters such as escape- and encounter-plane inclination, injection and arrival trajectory angles, and injection time were varied to determine their effects on injection-point coordinates and mission velocity-increment requirements. Trips of 150-, 225-, and 300-day duration were used to investigate the relations among velocity-increment requirements, departure date, trip time, communication distance, heliocentric transfer-plane inclination, and synodic period of departure. These data are compared with circular-coplanar results.</p>	<p>I. Knip, Gerald, Jr. II. Zola, Charles L. III. NASA TN D-1199</p> <p>(Initial NASA distribution: 2, Aerodynamics, missiles and space vehicles; 23, Launching facilities and operations; 24, Launching dynamics; 28, Missiles and satellite carriers; 46, Space mechanics.)</p>	NASA
<p>NASA TN D-1199 National Aeronautics and Space Administration. THREE-DIMENSIONAL SPHERE-OF-INFLUENCE ANALYSIS OF INTERPLANETARY TRAJECTORIES TO MARS. Gerald Knip, Jr., and Charles L. Zola. May 1962. 68p. OTS price, \$1.75. (NASA TECHNICAL NOTE D-1199)</p> <p>The method of analysis, for which equations are presented, employs arbitrary spheres to differentiate planetocentric and heliocentric motion. For a trip of fixed duration, planetocentric parameters such as escape- and encounter-plane inclination, injection and arrival trajectory angles, and injection time were varied to determine their effects on injection-point coordinates and mission velocity-increment requirements. Trips of 150-, 225-, and 300-day duration were used to investigate the relations among velocity-increment requirements, departure date, trip time, communication distance, heliocentric transfer-plane inclination, and synodic period of departure. These data are compared with circular-coplanar results.</p>	<p>I. Knip, Gerald, Jr. II. Zola, Charles L. III. NASA TN D-1199</p> <p>(Initial NASA distribution: 2, Aerodynamics, missiles and space vehicles; 23, Launching facilities and operations; 24, Launching dynamics; 28, Missiles and satellite carriers; 46, Space mechanics.)</p>	NASA
<p>NASA TN D-1199 National Aeronautics and Space Administration. THREE-DIMENSIONAL SPHERE-OF-INFLUENCE ANALYSIS OF INTERPLANETARY TRAJECTORIES TO MARS. Gerald Knip, Jr., and Charles L. Zola. May 1962. 68p. OTS price, \$1.75. (NASA TECHNICAL NOTE D-1199)</p> <p>The method of analysis, for which equations are presented, employs arbitrary spheres to differentiate planetocentric and heliocentric motion. For a trip of fixed duration, planetocentric parameters such as escape- and encounter-plane inclination, injection and arrival trajectory angles, and injection time were varied to determine their effects on injection-point coordinates and mission velocity-increment requirements. Trips of 150-, 225-, and 300-day duration were used to investigate the relations among velocity-increment requirements, departure date, trip time, communication distance, heliocentric transfer-plane inclination, and synodic period of departure. These data are compared with circular-coplanar results.</p>	<p>I. Knip, Gerald, Jr. II. Zola, Charles L. III. NASA TN D-1199</p> <p>(Initial NASA distribution: 2, Aerodynamics, missiles and space vehicles; 23, Launching facilities and operations; 24, Launching dynamics; 28, Missiles and satellite carriers; 46, Space mechanics.)</p>	NASA

